TANSZÉKVEZETŐ

SZAKDOLGOZAT TERVEZÉSI FELADAT

Drozdy András
villamosmérnök hallgató részére

Framework for the precision control of a laser beam

The Compact Linear Collider (CLIC) is a future high energy electron positron collider, which is the next step in examining the nature of matter. The CLIC is based on the two-beam acceleration concept, the high RF power to accelerate the main beam is extracted from a second high-intensity relativistic electron beam, the so-called drive beam that runs parallel to the main beam. The drive beam is decelerated to provide the RF power to accelerate the main beam itself. Photoinjector (PHIN) Lasers are used to achieve higher precision of the drive beam. The subject of this Thesis is to control this PHIN laser beam using phase coding.

- Describe the purpose and principle of the phase coding system of the Photoinjector (PHIN) laser based on the available literature
- Propose and implement a measurement method to enable precise adjustment of
    - the time delay in the phase coding system and
    - the amplitude balance of odd and even buckets of the phase coded laser beam
- Evaluate the precision of the two proposals and document your work

Tanszéki konzulens: Simon Csaba
Külső konzulens: Csatári Márta, CERN, Genf, Svájc

Budapest, 2011. március 10.

BUDAPESTI MŰSZAKI ÉS GAZDASÁGTUDOMÁNYI EGYETEM
Távközlési és Médiainformatikai Tanszék
Villamosmérnöki és Informatikai Kar

/ Dr. Henk Tamás /
egyetemi docens
tanszékvezető

Budapesti Műszaki és Gazdaságtudományi Egyetem
Villamosmérnöki és Informatikai Kar
Távközlési és Médiainformatikai Tanszék

1117 Budapest, Magyar tudósok krt. 2.
Telefon: +36 1 463 2448 Fax: +36 1 463 3107
E-mail: henk@tmit.bme.hu http://www.tmit.bme.hu

Budapest University of Technology and Economics
Faculty of Electrical Engineering and Informatics
Department of Telecommunications and Media Informatics

Drozdy András

FRAMEWORK FOR PRECISION CONTROL OF A LASER BEAM

The precision setup of phase-coding

EXTERNAL CONSULTANT

Csatári Márta

INTERNAL CONSULTANT

Simon Csaba

BUDAPEST, 2011

Table of contents

HALLGATÓI NYILATKOZAT

Alulírott **Drozdy András**, szigorló hallgató kijelentem, hogy ezt a szakdolgozatot meg nem engedett segítség nélkül, saját magam készítettem, csak a megadott forrásokat (szakirodalom, eszközök stb.) használtam fel. Minden olyan részt, melyet szó szerint, vagy azonos értelemben, de átfogalmazva más forrásból átvettem, egyértelműen, a forrás megadásával megjelöltem.

Hozzájárulok, hogy a jelen munkám alapadatait (szerző(k), cím, angol és magyar nyelvű tartalmi kivonat, készítés éve, konzulens(ek) neve) a BME VIK nyilvánosan hozzáférhető elektronikus formában, a munka teljes szövegét pedig az egyetem belső hálózatán keresztül (vagy autentikált felhasználók számára) közzétegye. Kijelentem, hogy a benyújtott munka és annak elektronikus verziója megegyezik. Dékáni engedéllyel titkosított diplomatervek esetén a dolgozat szövege csak 3 év eltelte után válik hozzáférhetővé.

Kelt: Budapest, 2011. 05. 13

....

Drozdy András

Abstract

In this thesis first the CLIC concept is introduced explaining the need for a new linear collider. The concept of two beam acceleration is described: the drive beam interleaving with delay loops, and the specific time structure of the electron beam needed for this. The purpose of CTF3 and the advantages of a photo injector as an electron source for the drive beam is explained.

A great advantage of the photo injector is that the special time structure required in the electron beam can be created in the laser beam. The fiber optic system at the head of the laser used to create the required time structure is described. This process is called phase-coding. The phase-coding requires the accurate adjustment of a delay line, and an optical attenuator, as these settings effect the timing accuracy and amplitude stability of the phase-coded beam.

A measurement method to determine the accuracy of the delay and amplitude balance is required for the adjustment of this delay and attenuation. Two methods are proposed: a frequency domain method using a spectrum analyzer and a time domain method using an oscilloscope.

Extensive measurements with both methods were carried out. Both methods proved to be accurate ways of determining the accuracy of the delay and amplitude balance. The frequency domain method is well suited for an easy setup of the system, and the time domain method was used for verification. Further developments are proposed to ensure that the timing and amplitude accuracy of the phase-coding is optimal.

Összefoglaló

Ebben a szakdolgozatban ismertetésre kerül a CLIC koncepciója, elmagyarázva az igényt egy új lineáris gyorsítóra. Bemutatom a két elektron nyalábos gyorsítás koncepcióját: a gyorsító elektronsugár késleltető hurkokkal történő önmagára lapolását, és az ehhez szükséges különleges idő struktúrát az elektronnyalábban. Taglalásra kerül a CTF3 szerepe és a photo-injektornak, mint elektronforrásnak, a használatának előnyei.

A photo-injektor egyik nagy előnye, hogy az elektron nyaláb szükséges időstruktúráját már a lézernyalábban létre lehet hozni. Az ehhez szükséges a lézerrendszer elején alkalmazott üvegszál optikás rendszert részletesen leírom. Ennek az időstruktúrának a létrehozását fáziskódolásnak hívjuk. A fáziskódolás egy késleltetés és egy optikai csillapító finom beállítását igényeli, mivel ezek a beállítások közvetlen hatással vannak a fáziskódolt nyaláb időzítési viszonyainak pontosságára és amplitúdó stabilitására.

Ezért szükséges egy mérési módszer a késleltetés és amplitúdó egyensúly pontosságának meghatározására, a késleltetés és csillapítás beállítása végett. Két módszert javasolunk egy frekvencia tartománybelit egy spektrum analizátor segítségével és egy időtartománybelit egy oszcilloszkóp segítségével.

Mindkét módszerrel végeztem méréseket. Mindkettő jó módszernek bizonyult a késleltetés és amplitúdó egyensúly pontosságának meghatározására. A frekvencia tartománybeli módszer jól alkalmazható a fáziskódolás könnyű beállítására, az időtartománybeli módszerrel pedig ellenőrzésre használtuk. További fejlesztéseket javasolunk a fáziskódolás időzítési és amplitúdó pontosságának növelésére.

1. The CLIC concept

The particle physics of the 21st century aims to probe deeper into nature of matter, beyond the standard model. Major experiments of accelerator laboratories such as CERN are all aimed in this direction [1].

The TeV energy range is expected to open up a whole new range of physics, in particular that connected with the origin of particle masses. This new physics might include an elementary Higgs boson, but most physicists would expect the new physics to be more complex, perhaps including new spectroscopy of supersymmetric particles or other excitations [1].

The first exploration of the TeV energy range will be made with the Large Hadron Collider (LHC), and what it will find cannot be foreseen. However, it is impossible to expect that experiments at the LHC will actually answer all the questions concerning this new physics. For example, research physicists are likely to want more information about any kind of Higgs boson than what the LHC can tell us. Moreover, if nature chooses supersymmetry, it can be expected that the LHC will reveal a number of supersymmetric particles but not all of them. If nature chooses to replace an elementary Higgs boson by new strong interactions, the hints that the LHC would provide should be followed up by other experiments. Many of the open questions may best be addressed by a lepton–antilepton collider [1]. The LHC is a discovery machine; a machine for precise measurements is required. CLIC (Compact Linear Collider) is a high energy electron positron collider, designed to fulfill this demand.

The highest energy electron positron collider to date is LEP with an energy of 209 GeV in the center of mass system. In this system the circulating particles lost 3.4% of their energy per turn due to synchrotron radiation. A powerful RF system provides a circumferential voltage of 3.6 GeV to compensate this effect [2]. Since the energy loss due to synchrotron radiation is proportional to the fourth power of the energy and inversely proportional to the radius, a circular electron positron collider in the TeV range is not feasible, this is the prime reason for CLIC being a linear collider.

Acceleration in a linear collider is achieved by using disc loaded RF accelerating structures. RF power is guided into a cavity, through which the electron beam travels. The cavity is shaped so that the phase velocity of the RF wave is equal to the velocity of the electron beam, so that the electric field of the RF wave can accelerate the electrons [3].

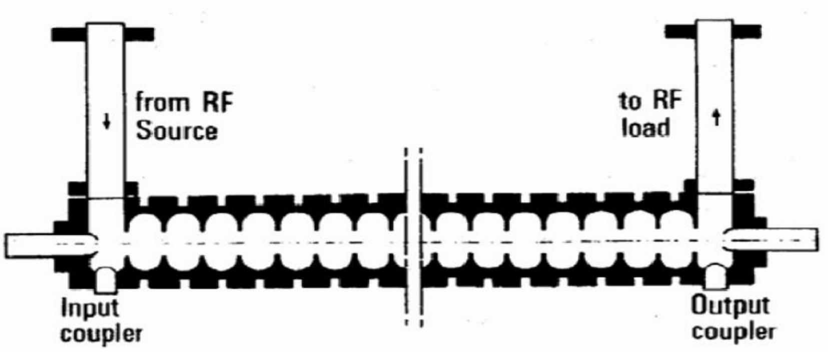

Figure 1.1.: Accelerating structure schematic [3]

These RF structures can be divided into two basic types superconducting and room temperature. Superconducting RF structures are more efficient, and can be used to accelerate longer pulse trains, however they have a smaller accelerating gradient (around 20-30 MV/m). Because of the large accelerating gradient required to achieve the high energies in a reasonable length, CLIC uses room temperature accelerating structures, to achieve a nominal accelerating gradient of 100 MV/m.

Figure 1.2.: A superconducting accelarating structure [2]

Figure 1.3.: A room temperature accelerating structure [2]

A large amount of RF power is required along the whole length of the accelerator, CLIC tackles this issue with a novel two beam accelerating scheme. The power needed is produced centrally and used to accelerate a second electron beam the drive beam. The drive beam travels alongside the main beam in the tunnel, and is converted through power extraction structures (PETS) to RF which powers the accelerating structures of the main beam. By interleaving the bunches of the drive beam through a delay loop and combiner rings before entering the tunnel, this scheme allows high peak RF power at 12 GHz to be created locally. This leads to a compact design where there are no active components or additional structures required along the tunnel.

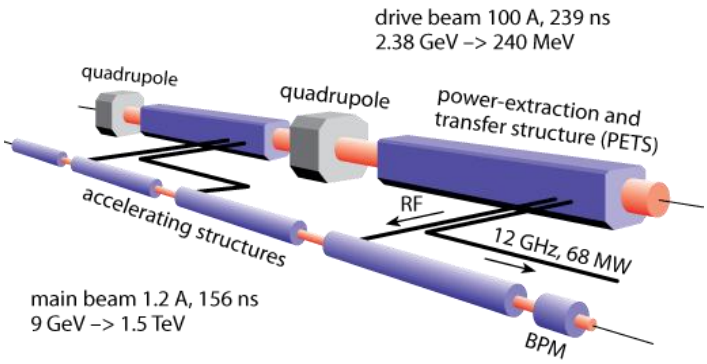

Figure 1.4.: The two beam acceleration scheme [4]

The CLIC study aims at collider with center of mass energy from 0.5 TeV to 5 TeV, with 3 TeV being the nominal value. The following will be written with the 3 TeV scenario in mind. It is important to note that many CLIC parameters are subject to change as the work progresses. The conceptual design report is expected this year.

The main electron beam is created with a photo injector and then after acceleration to 9 GeV is injected into the main linac (linear particle accelerator). The bunch spacing of the main beam is 12 GHz.

The concurring technologies for the drive beam injector are a photo injector or a thermionic injector. The drive beam is accelerated to 2.38 GeV along the drive beam linac with 0.5 GHz bunch repetition rate, which is increased by interleaving the bunches, to 1 GHz then in the two combiner rings to 12 GHz, to be used to power the 12 GHz main beam. The delay loop used and the combiner ring require a special time structure to achieve the 12 GHz equally spaced bunches of the drive beam.

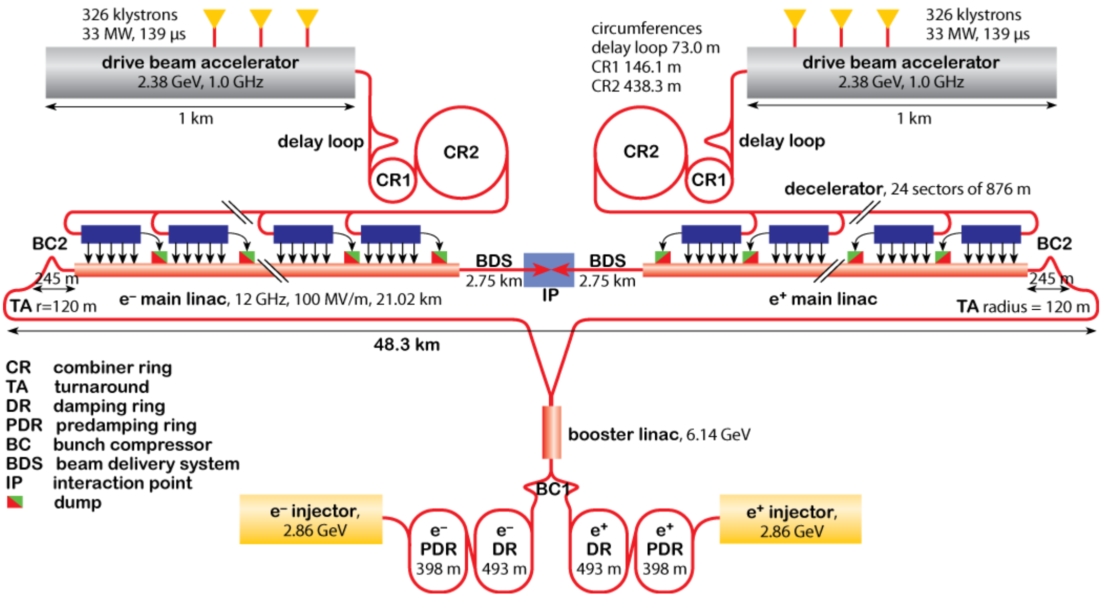

Figure 1.5.: CLIC plans [5]

The high accelerating gradient of 100 MV/m allows CLIC 3 TeV to be built with a length less than 50 kilometers for the main linac. By comparison the LEP (large electron positron collider) was a circular collider with a total energy of 45 GeV, and with a circumference of 27 kilometers. The former LEP tunnel now accommodates the LHC.

1.1 CTF 3 – The study so far

At the moment the some of the most important parts of the CLIC study are investigated in CLIC test facility 3 (CTF3). In CTF3 power production, 12 GHz beam combination and the two beam acceleration scheme are being tested.

The drive beam used is generated with a thermionic gun. A thermionic gun is a continuous electron source, so the beam it creates has to go through a bunching system to produce the short electron bunches required.

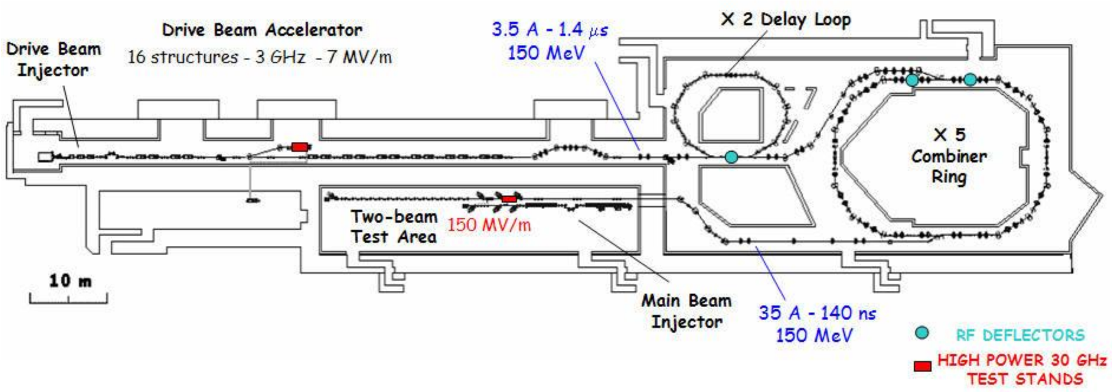

Figure 1.6.: The CLIC Test Facility 3 [6]

The power from the drive beam extracted through the so called PETS (Power Extraction Structure) by deceleration of the beam. The main beam produced by a photo-injector is then accelerated using this power in the TBTS (Two Beam Test Stand) accelerating structures.

The nominal CLIC bunch repetition rate is 468.5 MHz [7] which is then interleaved to approximately 15 GHz, but CTF3 uses 1.5 GHz which is then interleaved times two in the delay loop and times four in the combiner ring, resulting in a pulse repetition rate of 12 GHz, which corresponds to the CLIC accelerating structures. The two beam test stand has already demonstrated the 100 MV/m acceleration gradient necessary for CLIC.

1.2 Photo injector

A photo injector is a special electron source working on the principle of photo-emission. A typically multi alkali cathode is placed in vacuum and illuminated by a laser of light, where the frequency of light is chosen, so that photoemission can occur. A DC or RF field is applied to the cathode to pull the electrons out thus forming a beam (figure: 1.7.). The light source is typically a pulsed laser source. The timestructure of the laser beam determines the bunch structure produced.

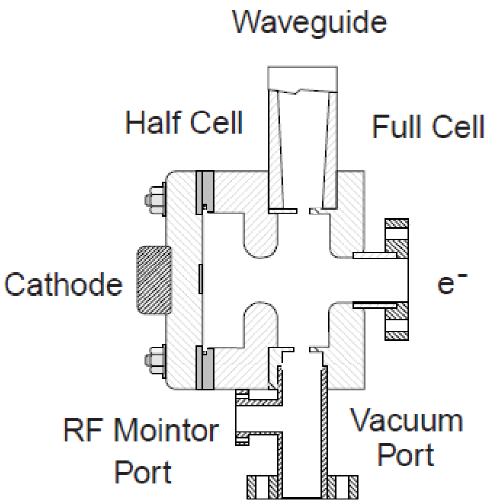

Figure 1.7.: A photo injector cavity - a 1.6 cell RF gun [8]

Although the baseline design of CTF3 and CLIC assumes a thermionic drive-beam injector, an option for a photo-injector is kept open because of its advantages. [9]

In the thermionic gun manipulating the time structure of the electron beam is hard task for the bunching system. The time structure required involves a train of pulses at a given frequency of which certain groups are required to be delayed 180° in phase. This manipulation of the time structure of the beam is referred to as phase-coding. In the thermionic gun this cannot be perfectly implemented. The switching is not instantaneous the pulses in phase gradually decrease in magnitude while the pulses out of phase gradually increase in amplitude, resulting in unwanted pulses, called satellites. This unwanted charge can cause considerable radiation problems and efficiency loss, and causes transient beam-loading in the CLIC main beam. [9]

One of the major advantages of using a photo injector is the flexibility in manipulating the time structure of the beam in the laser directly before the production of the electrons. Laser beams can be switched almost instantaneously thanks to recent telecommunication development. Further advantages of the photo injector are: smaller transverse and longitudinal emittance and thus easier beam transport and bunch length manipulation. [9]

In CTF3 main beam is created using the photo-injector CALIFES. The same laser is also used to investigate the possibility of using a photo-injector to generate the drive beam, for this the PHIN photo-injector is used. The nominal beam for CTF3 drive beam has an average current of 3.5 A, at 1.5 GHz bunch repetition frequency and a pulse length of 1.5 μs, with 2332 10 ps long bunches). This can be produced in the gun of PHIN, which has 2.5 cells and works at an RF frequency of 3 GHz [10]. The cathode is a Cs_2Te which offers quantum efficiencies (QE) of over 1.5% for several months, and can be used with UV wavelength of 262 nm [10].

A fiber-optic solution at the beginning of the laser amplification system is used to achieve phase-coding. The subject of this thesis is to develop a method for the precision setup of the timing and amplitude balance of the phase-coding system.

2. The LASER

The laser system is custom built specifically for this application (see figure 2.1). The front end of the system was manufactured by HighQ laser, including the oscillator and the preamplifier, which are synchronized to the RF frequency of the CTF3 machine. The laser medium is Neodymium doped ytterbium-lithium-fluorite (Nd:YLF and used at 1047 nm wavelength emission. The preamp is a diode pumped slab amplifier. The laser light in these stages is quasi-continuous-wave (quasi-cw); consisting of 5.5 ps pulses at a repetition rate of 1.5 GHz with 10W of average power.

The IR light is then amplified by two diode pumped laser amplifiers (see figure 2.2.). These are 5 fold side diode pumped Nd:YLF rod amplifiers . These amplifiers are pumped for a few hundred microseconds, during which time the output slowly reaches a steady-state. Only the end of pulse train is used, to take advantage of the steady state operation. This is achieved by selecting a desired length of pulsetrain with a Pockel's cell from the end of the amplified pulse train. The system is designed so that the input of the amplifiers is sufficient to reach saturation. This is useful because the marginal gain of increasing the input power to the amplifier is very small, thus the amplifiers have a stabilizing effect to slow input variations.

If very short pulse trains or single pulse are desired the beam can be sent through further two Pockel's cells called pulse pickers. A two cell scheme is required to enable one of them to open, the other to close very fast in between consecutive pulses.

The photocathode used for high charge production is made out of cesium tellurite Cs_2Te so the light needs to be converted to UV for the photo-emission process to work. This is achieved by first converting the light to 523 nm by doubling its frequency in a conversion crystal (for example: KTP Potassium Titanium Oxide Phosphate). This green light is then frequency doubled again to create the necessary UV, this can be done with an ADP (Ammonium Dihydrogen Phosphate) or KDP (Potassium Dihydrogen Phosphate) crystals for example.

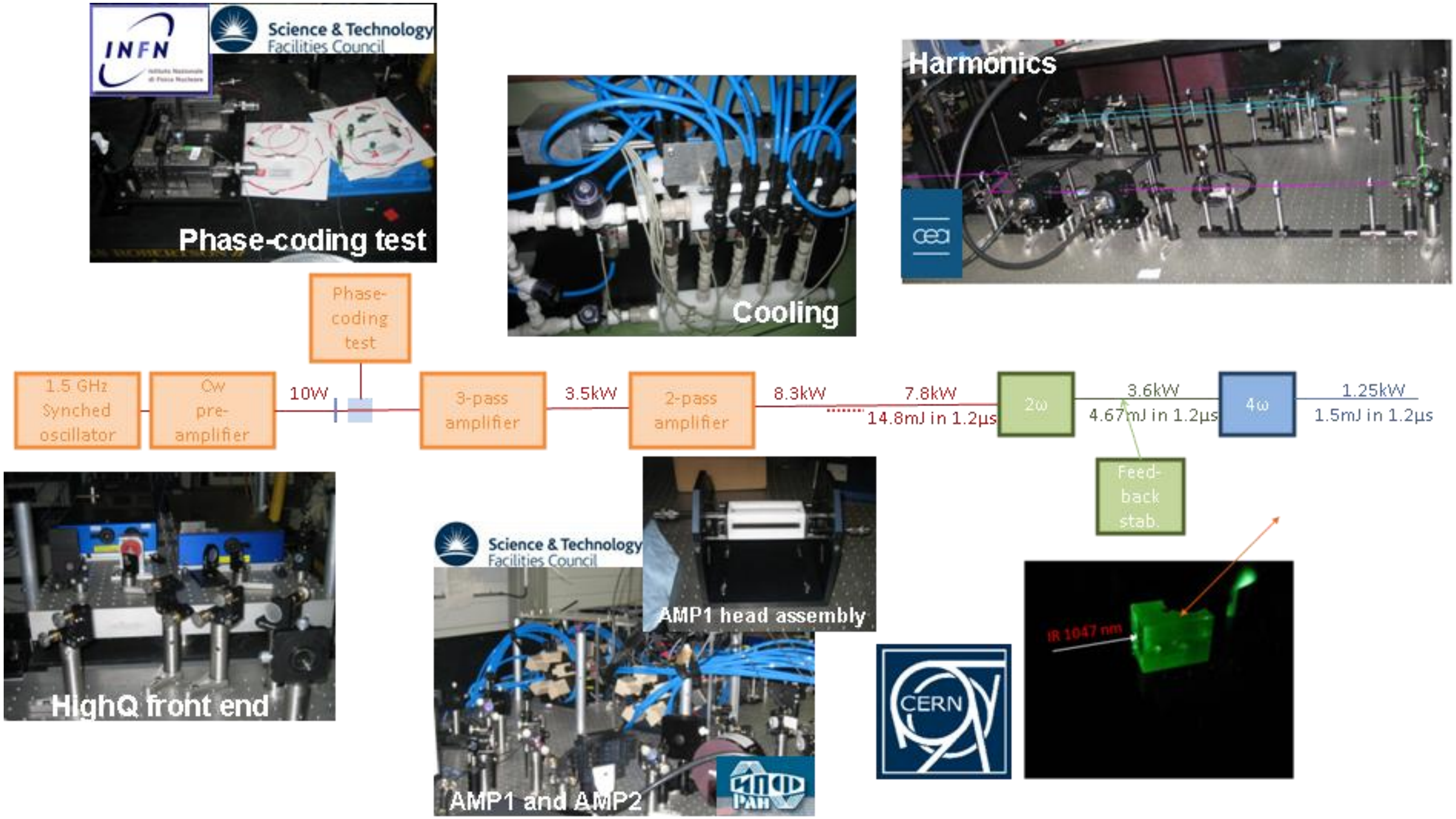

Figure 2.1.: Layout of the laser system [11]

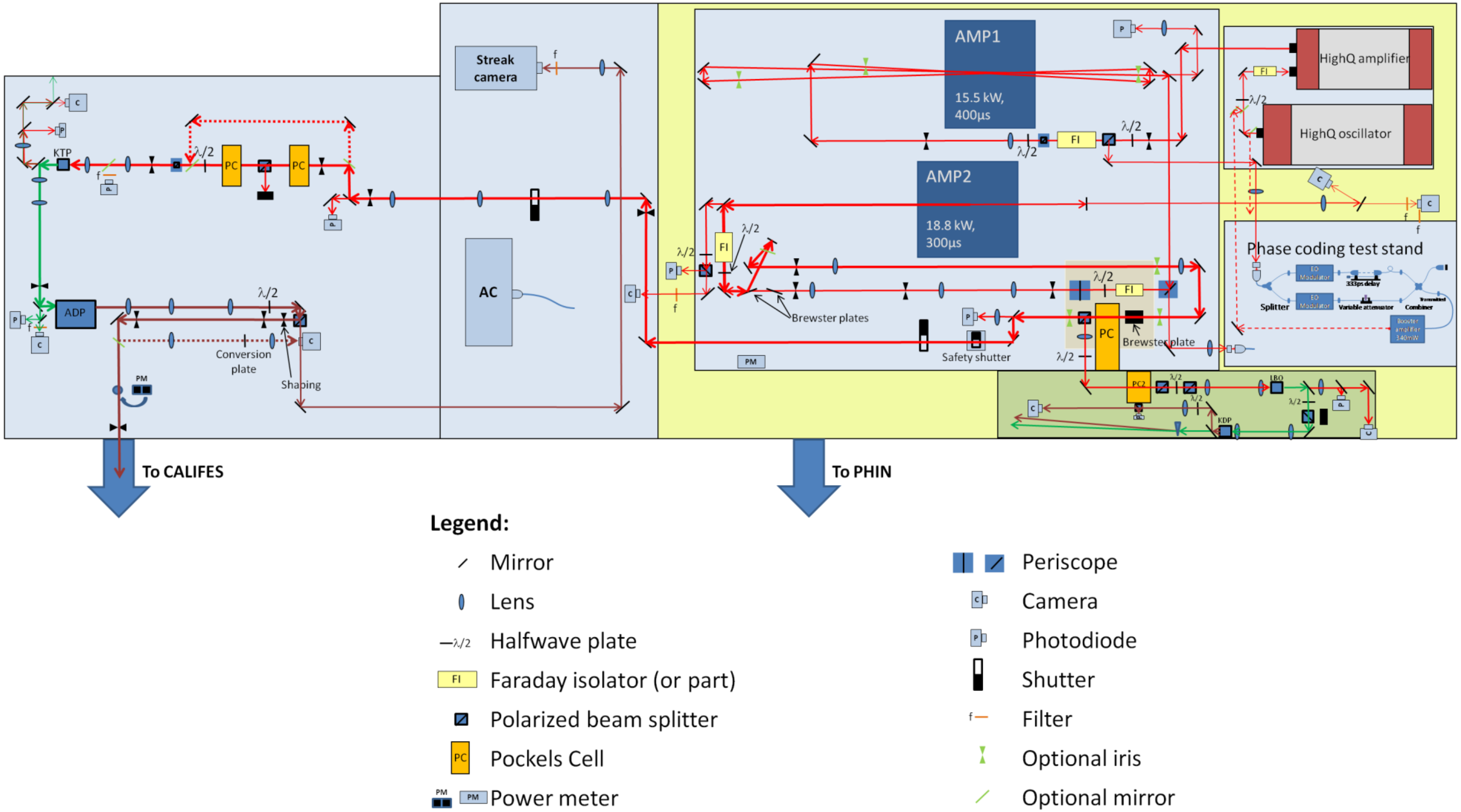

Figure 2.2.: Layout of the laser system

3. Phase-coding

3.1 The purpose of phase-coding

As previously stated the drive beams power density is increased by interleaving it with itself through the use of a delay loop and combiner rings. The delay loop works on the principle of using a transverse RF deflector to send split the beam along two beam paths, and then uses the same principle to combine the beams again.

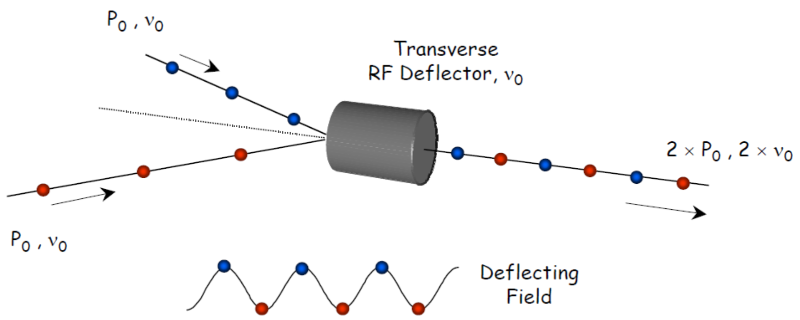

Figure 3.1.1.: A transverse deflector [7]

This can be achieved by defecting the bunches in phase with the deflector field one way and the ones 180° out of phase to go straight. This technique results in a clean extraction of the bunches if the phase is accurate. A series of bunches in phase with the RF field is called an odd sub-train, and a series of bunches 180° out of phase is called an even sub-train.

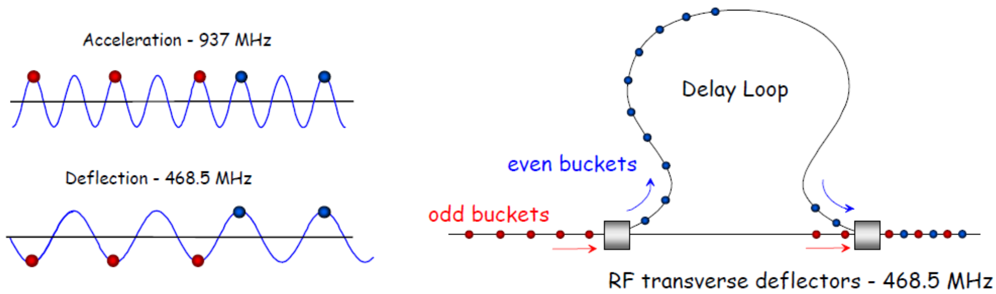

Figure 3.1.2.: The delay loop operation [7]

The drive beam consists of a series of odd and even sub-trains. The even sub-trains are deflected towards the delay loop the odd ones travel the shorter path, the delay is chosen such that the consecutive odd and even sub-trains are interleaved, doubling the bunch repetition frequency, and halving the fill factor. In the combiner ring the pulses, each consisting of an odd and an even sub-train, are combined even further: four consecutive pulses are interleaved to quadruple the frequency. The resulting pulse train consists of a number of pulses equal to the number of decelerating sections along the main linac. In these decelerating sections the RF power for the acceleration of the main beam is produced with PETS (Power Extraction Structure). In CTF3 1.5 GHz is interleaved to make 12 GHz, times 2 in the delay loop and times 4 in the single combiner ring.

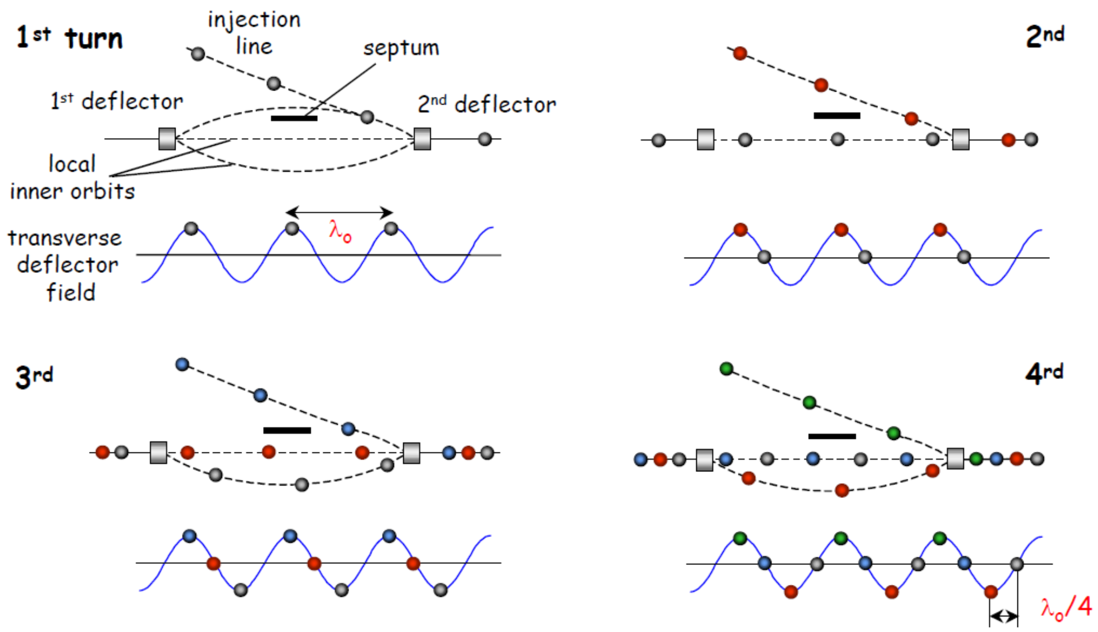

Figure 3.1.3.: The operation of transverse RF deflectors used in the combiner rings [12]

Similarly in CLIC, the bunch repetition frequency of 500 MHz will be increased to 12 GHz in by interleaving times 2 in the delay loop and times 3 and times 4 in the combiner rings. Creating the odd- and even sub-trains directly in the laser allows very high precision switching, when photo-injector option is used.

3.2 The phase-coding fiber optics

A small portion of the preamplifier output is diverted to the phase-coding test stand phase-coding. In the first PHIN run this year the phase-coding was integrated into the laser system for the first time. The phase-coding was driven with the preamp output and joined back into the system through the booster amp to the input of amplifier 1.

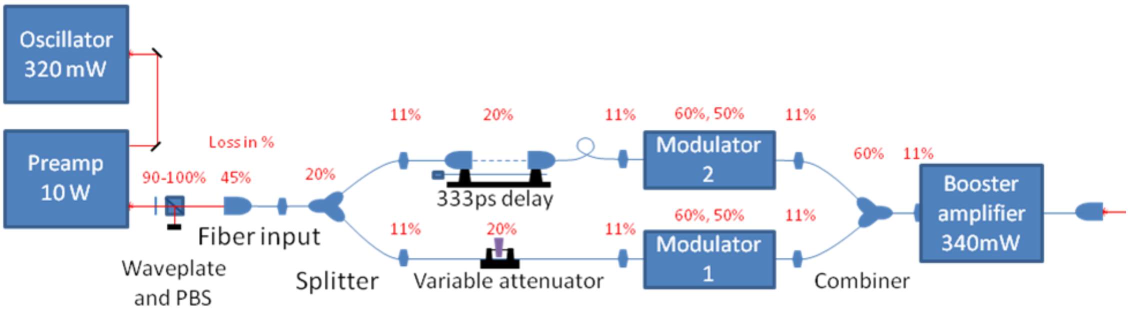

Figure 3.2.1.: Phase-coding scheme

The phase-coding is implemented at the front end of the laser system because here the power is sufficiently small for fiber optic modulators to handle.

This solution using fiber optic modulators was chosen, because conventional Pockel's cells (which are used in other parts of the system) work with much higher switching voltage of few kV's. To be able apply such voltages to the electro-optic crystals with the necessary switching speeds would have required far more power and thus more complicated electronics. The fiber optic modulators are smaller in size and require a switching voltage of only a few volts but have limited power input handling.

The laser light at the front end of the system is qcw (quasi-continuous wave), so it consists of 5.5 ps wide pulses with a repetition rate of 1.5 GHz. The laser light is focused onto the input of a fiber through a lens system. The light is then split into two, using a polarization maintaining splitter. The splitter has two output arms, one of which is delayed with a variable delay line, consisting of an air gap with a size adjustable by screw. This arm is delayed 333 ps compared to the other to create the required 180° phase-shift. The other arm contains a variable attenuator to match the attenuation of the delay arm. Then the electro-optic modulators are used to switch the transmission between 0% and 100% with a fill factor of 50%.

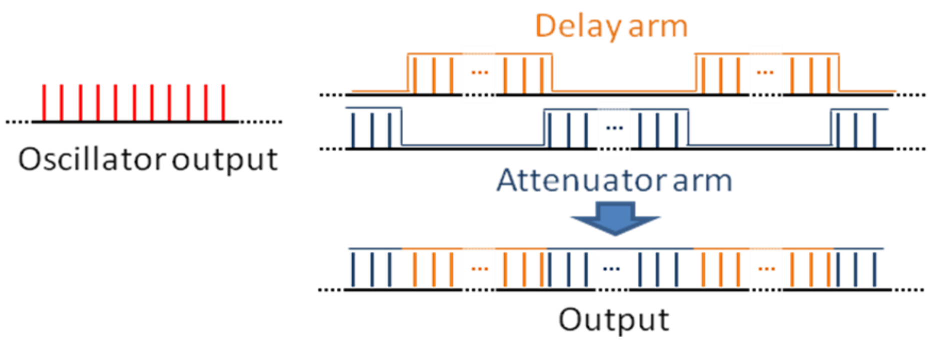

Figure.3.2.2.: The phase-coding time structure

The output of the modulators is then added using a non-polarizing beam splitter in reverse. This results in a signal in which every second sub train is delayed by 180° in phase (333 ps in time). Later in the laser system the qcw signal is only amplified for a few hundred µs, from this amplified part 8 sub trains are cut out with a Pockel's cell to be used for PHIN. In this manner the required phase coded time structure is created.

Originally the phase-coding was planned to be directly connected to the oscillator output however by using the preamp as well the amount of power to the modulators could be always set to be just under the damage threshold. The booster amplifier would have seeded the preamp, but due to the great beam quality of the booster amplifier output, it can be used to power amplifier 1 directly, despite its low power.

All fibers used in the system are single mode, panda type polarization maintaining fibers, with a core diameter of 6 µm and a clad diameter of 125 µm. The used splitter is 50-50% pigtail style non-polarizing splitter from Ozoptics. The variable delay (ODL-100) also from Ozoptics only has a delay range of 330 ps this range is unfortunately insufficient to guarantee that the delay can be set to 333 ps, it is important to note that due to the differences in fiber length between the two arms the delay between them does not come solely from the air gap. The solution to this is that a short fiber introducing a delay of about 220 or 440 ps can be inserted if necessary (7/13 cm). The variable attenuator also from Ozoptics (BB-700) works on a principle of collimating the beam with two lenses and physically blocking a part of the beam with a screw. The combiner is not a polarizing combiner so it combines regardless of polarization, but inherently has a loss of more than 50%.

The two modulators are manufactured by Photline technologies, the newer model is: NIR-MX-LN-03, the older model is practically equivalent. The modulators recommended maximum CW input power is 100 mW. The modulators are $LiNbO_3$ Mach-Zender intensity modulators. Such a modulator splits the input light into two paths, phase shifts one of the paths, the two paths rejoin, and the output intensity is modulated by their constructive or deconstructive interference. Thus the output of a modulator is a sine function of the applied voltage (see figure 3.2.3.). A bias voltage is required to set the operating point of such a modulator. This bias voltage and power supply voltage is provided by an MBC benchtop bias controller, this controller also has a feedback system to compensate for the drift of the operating point. This feedback does not work well with our fill factor of 50%, and because the drift was found to be not very significant, this function was not used. It is important to note that these modulators only work with a single polarization. The required RF modulating signal was provided by an AC amplifier (DR-PL-10-MO-LR) which, designed for short pulses, this is not the case in our application as we have a 50% fill ratio square wave however it provides the fast rise times necessary efficiently and will also dampen variations on the driving voltage.

The input of the amplifier was provided by a custom made electronic made at CERN designed to fit the phase-coding to local timing signals. This box produces two 50% fill ratio square waves both in the same phase, and also houses the RF amplifiers to reach the required drive voltage for the modulators. The two modulators are used in opposite operating point; QUAD+ and QUAD-.

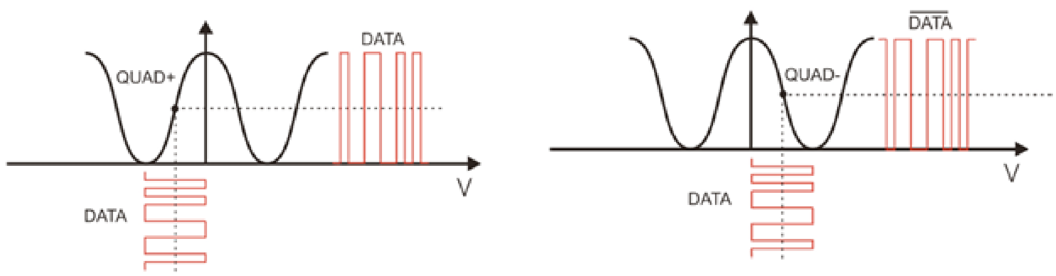

Figure 3.2.3.: Modulator transmission vs. drive voltage – modes of operation [13]

As the modulating singles can be used with one off and the other on, only 333 ps relative delay is required between the two arms. This delay and an appropriate common delay is setup so that the modulators switch in between laser pulses. The two required delays to the modulators are setup by varying the cable length carrying the signal to the modulators. This method was chosen because it provides a very stable delay without further active electronics. Unfortunately setting this is very time consuming and requires cable cuts with 100ps accuracy. The amplitude of the modulation is set by changing gain of the amplifiers.

3.3 The task at hand

The phase-coding requires the fiber optic attenuator and delay to be set with high accuracy. (The time structure can be seen on figure 3.2.2.). The stability requirements of the resulting phase-coded electron beam are 0.1% RMS in intensity and less than 1 ps RMS timing error/jitter. Both quantities can are directly inherited from the laser beam properties. The timing jitter originates from the synchronization of the oscillator and is almost constant throughout the laser system with about 0.5 ps RMS jitter. **The prime goal of this work is to develop a method to adjust the delay as accurately as possible so as to cause virtually no increase in timing jitter.**

The amplitude noise of the laser system, changes throughout the system, the amplitude noise in the oscillator and preamplifier are suppressed at low frequencies in amplifier 1 and 2, due to the fact that these amplifiers are used in saturated steady state. This means that increasing the input power on these amplifiers only marginally increases the output power. As the passes through the harmonic stages any instability is increased due to the nonlinear nature of the conversion processes. At first estimate this causes the amplitude noise to double on each conversion stage. The noise of the laser beam going to the photo-injector was measured at 1% RMS in the UV. However the since the acceptance test of the oscillator, Q switching instabilities have appeared at ~400MHz region. This is a phenomena is known to appear in high repetition rate passively mode-locked lasers [14], often due to degradation of the optics. This has a huge effect on the stability of the laser beam, before the latest oscillator and preamp service, the noise was as high as 8% after the preamplifier increasing to 14 and 22% in amplifiers 1 and 2. After the service this noise has decreased to less than four percent, at the preamp. This problem will be hopefully fixed soon and the stability of the laser is to be further increased through a feedback system in the near future. Despite this noise performance of the laser at the moment the added amplitude noise of the phase-coding is important, for the demonstration of the phase-coding.

Thus he phase coding has to achieve a good amplitude balance between odd and even sub trains compared to 0.1%.

So the second goal of this work is to achieve the best possible amplitude balance between the odd and even sub trains of the phase coded laser beam. This is made harder by the relatively high amplitude noise that is observable on the laser beam at the time.

4. Two methods for alignment of the phase-coding

4.1 Introduction

The goal is to give an easy and accurate method for adjusting the delay and amplitude balance of the phase-coding system. It is a great advantage if used method gives instant visual feedback to the laser operator, as this is the method used throughout the laser system for alignment and other purposes. It is of interest to us that while alignment procedures can be automated using picomotors to move the mirrors with even the beam position being monitored automatically, it is usually preferred to do these procedures manually if high precision is needed. Similarly the used optic delay can be ordered with a picomotor to adjust the delay, however this does not provide a higher resolution than the manual version and once the system is set further adjustment is not necessary.

First the optical signal has to be measured this is most accurately done by photodiode. Our highest bandwidth photodiodes are the New Focus 1024 with an impulse response of 12 ps FWHM, and the New Focus 1014 with a 3 dB bandwidth of 45 GHz. The New focus 1024 is optimized for time domain measurements and the 1014 is optimized for frequency domain measurements, however they were both found to be well suited for both. They are particularly practical for this propose because they have fiber optic inputs. Knowing this we can clearly see that the 5.5 ps laser pulses cannot be fully resolved with these detectors. For high temporal resolution an autocorrelator is used for pulse width measurement.

4.2 The problem

While the delay can be roughly set using the digital oscilloscope, this does not provide an accurate, measurement because of the timing jitter already present. For instance the first pulse in a sub-train can be one picosecond late compared to the average phase of all the other pulses, due to timing jitter; this would result in our delay being a whole picosecond off. Furthermore the oscilloscope has to trigger at a phase shift this can not be ensured on a balanced train, so a single trace has to be recorded and a phase shift has to be found in the trace, this can be very tedious. Of course these difficulties can be overcome as described later.

It can be also possible to check the output signal in the frequency domain. The Fourier transform of a train of Gaussian pulses, consists of spectral lines at multiples of 1.5 GHz and of course at DC. If a part of this signal is phase shifted other frequency components also appear, depending on the sub train length. By varying the phase shift the spectrum changes only slightly. The resulting spectrum of a phase-coding with the correct delay and with a 30 ps offset on the delay, can be seen in figure 4.2.1. and in figure 4.2.2. These graphs were numerically calculated by using FFT in MATLAB.

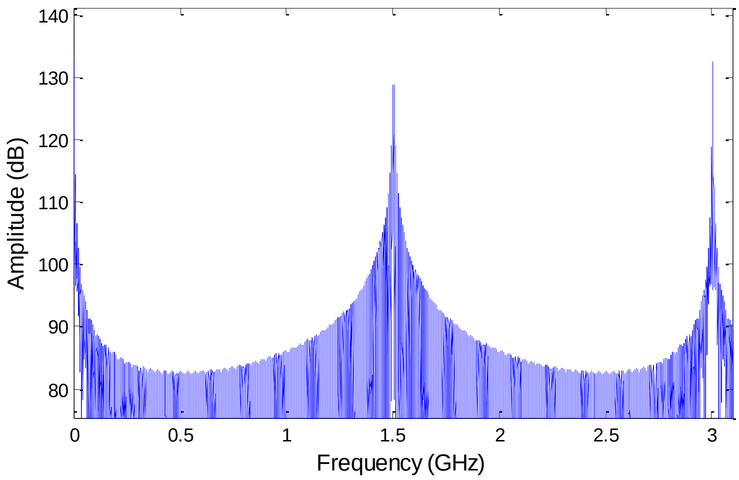

Figure 4.2.1.: Spectrum of phase coded beam

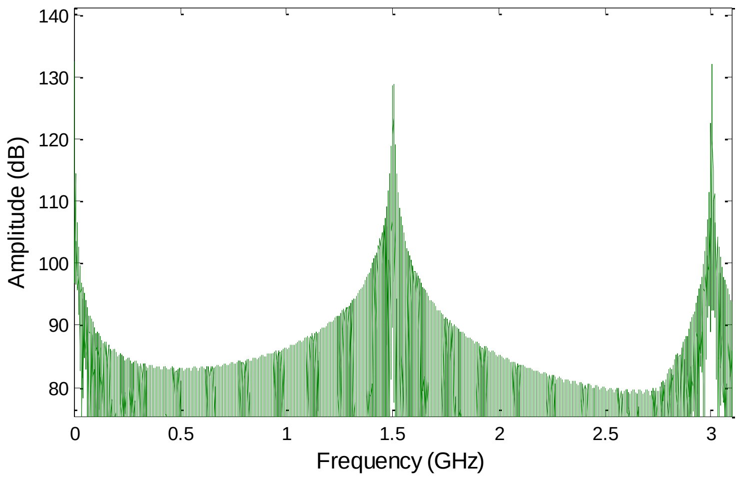

Figure 4.2.2.: Spectrum of phase coded beam with 30 ps error

4.3 The frequency domain method

If the RF input to the modulators is turned off, both modulators will be constantly at a QUAD operating point, at 50% transmission. This results in the output of the phase-coding being a train of equally spaced pulses with a repetition rate of 3 GHz. If the delay is set incorrectly every second pulse will be phase shifted compared to this 3 GHz. This is very useful for us, because in this mode of operation a small error in the delay results in a significant change in the spectrum.

The Fourier transform of a Gaussian of form (1) is a Gaussian of the form of (2)

$$f(t) = a \cdot e^{-\frac{t^2}{2c^2}} \quad \textbf{(1)}$$

$$\hat{f}(\omega) = a \cdot c \cdot e^{-\frac{c^2\omega^2}{2}} \quad \textbf{(2)}$$

The Fourier transform of a comb function (3) is a comb function (4).

$$g(t) = \sum_{k=-\infty}^{+\infty} \delta(t - kT) \quad \textbf{(3)}$$

$$\hat{g}(\omega) = \sum_{k=-\infty}^{+\infty} \delta(\omega - k\omega_0) \quad \textbf{(4)}$$

A series Gaussian pulses is the convolution of a Gaussian pulse and a comb function, so the Fourier transform is the multiplication of the two:

$$F_{train} = F\{f(x) * g(x)\} = \sqrt{2\pi} \cdot \hat{f}(\omega) \cdot \hat{g}(\omega) \quad \textbf{(5)}$$

$$F_{train} = \omega_0 \cdot a \cdot c \cdot e^{-\frac{c^2\omega^2}{2}} \sum_{k=-\infty}^{+\infty} \delta(\omega - k\omega_0) \quad \textbf{(6)}$$

In our case phase-coding we take two of these trains delay one of them and then add them together then their Fourier transform will be:

$$F_{sum\ train} = F_{train} + e^{-i \cdot \varphi \cdot \frac{\omega}{\omega_0}} \cdot F'_{train} \quad \textbf{(7)}$$

$$F_{sum\ train} = \left(a + a' \cdot e^{-i \cdot \varphi \cdot \frac{\omega}{\omega_0}} \right) \cdot \omega_0 \cdot c \cdot e^{-\frac{c^2\omega^2}{2}} \sum_{k=-\infty}^{+\infty} \delta(\omega - k\omega_0) \quad \textbf{(8)}$$

Where the amplitude of the trains are a and a', and the second train is delayed by φ.

If there is no delay $(\varphi = 0^\circ)$ then the spectrum consists of the DC component and 1.5 GHz and its multiples. As the delay increases to 180° the spectral line at 1.5 GHz decreases and the spectral line at 3 GHz increases, until the spectral line at 1.5 GHz disappears. The odd multiples of 1.5 GHz also disappear at $(\varphi = 180^\circ)$, giving us the spectrum of a 3 GHz repetition rate train of Gaussians, as expected.

The absolute value of the Fourier transform is:

$$\mathrm{Mag}\{F_{\text{sum train}}\} = \omega_0 c \cdot e^{-\frac{c^2\omega^2}{2}} \sum_{k=-\infty}^{+\infty} \delta(\omega - k\omega_0) \cdot \sqrt{\left(a + a' \cos\frac{\omega\varphi}{\omega_0}\right)^2 + \left(a' \cdot \sin\frac{\omega\varphi}{\omega_0}\right)^2} \quad \textbf{(9)}$$

If $a = a'$ this can be further simplified to:

$$\mathrm{Mag}\{F_{\text{sum train}}\} = \sqrt{2 + 2\cdot\cos\left(\frac{\omega\varphi}{\omega_0}\right)} \cdot \omega_0 c \cdot e^{-\frac{c^2\omega^2}{2}} \cdot \sum_{k=-\infty}^{+\infty} \delta(\omega - k\omega_0) \quad \textbf{(10)}$$

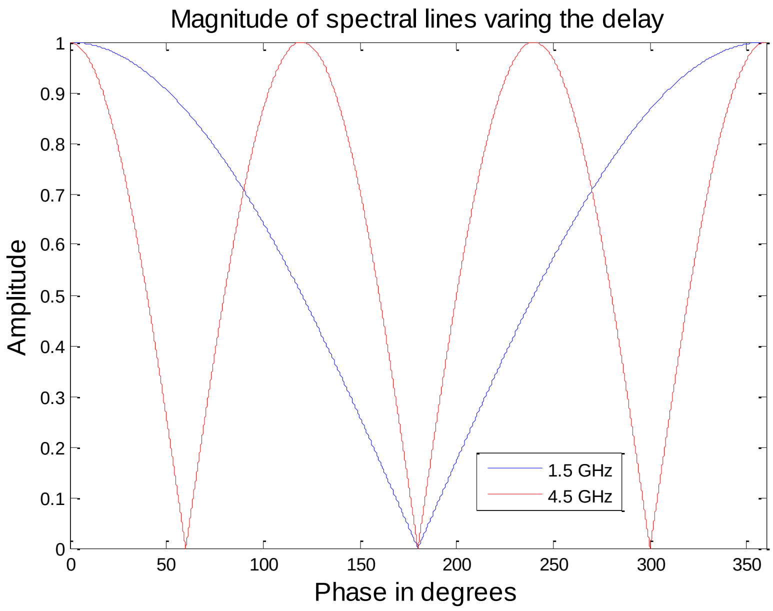

Figure 4.3.1.: Magnitude of spectral lines

The amplitudes are compared to the maximum of the 3 GHz peak and $e^{-\frac{c^2\omega^2}{2}}$ is considered to be constant in this range. This assumption is valid because the width of the Gaussian envelope of the spectrum is 146 Hz (FWHM), this is determined by the pulse length.

Changing the amplitude of the delayed sub pulse train pulse, changes the size of the spectral lines at 1.5 GHz or any of its multiples in the same way: the amplitude increases linearly to the unbalance regardless of the direction in which the arms are unbalanced. The effect of time delay on the spectrum is greater if we look at higher multiples of 1.5 GHz, unlike the effect of the amplitude unbalance between the arms.

4.3.1 The procedure

The laser signal can be measured anywhere along the fibers before the booster amp, simply by disconnecting the fiber of interest and connecting it to the photodiode, usually using an intermediate fiber. The photodiode is connected to the spectrum analyzer or oscilloscope directly, requiring no cable.

1. The delay is set roughly with the oscilloscope, using an unbalanced train with modulators on, this allows the oscilloscope to trigger at the change in amplitude between odd and even sub-trains. The signal before the booster amp is used.
2. The amplitude balance is restored by adjusting the fiber optic attenuator.
3. Then the delays of the RF signals to the modulators are checked.
4. The operating point of the modulators is also adjusted.
5. The modulation is turned off. The signal before the booster amp is connected to the spectrum analyzer through the photodiode.
6. The fiber optic attenuator is adjusted; first increasing the attenuation, if the peak at 4.5 GHz decreases the attenuation is further increased until the peak at 4.5GHz is minimized. If the peak at 4.5 GHz starts to increase, then the attenuation is instead increased until the peak is minimized.
7. Then the time delay is adjusted in a simulate manner, to decrease the peak at 4.5 GHz on the oscilloscope.
8. Steps 6 and 7 are repeated until noise floor is reached.
9. Then the modulation is turned back on to check amplitude balance with oscilloscope.

4.4 The time domain method

As previously mentioned the delay can also be measured by oscilloscope, the best oscilloscope available in the lab is the LeCroy Serial Data Analyzer SDA18000. This oscilloscope has a bandwidth of 18 GHz our photodiode (the New Focus 1024) has an impulse response of 12 ps FWHM.

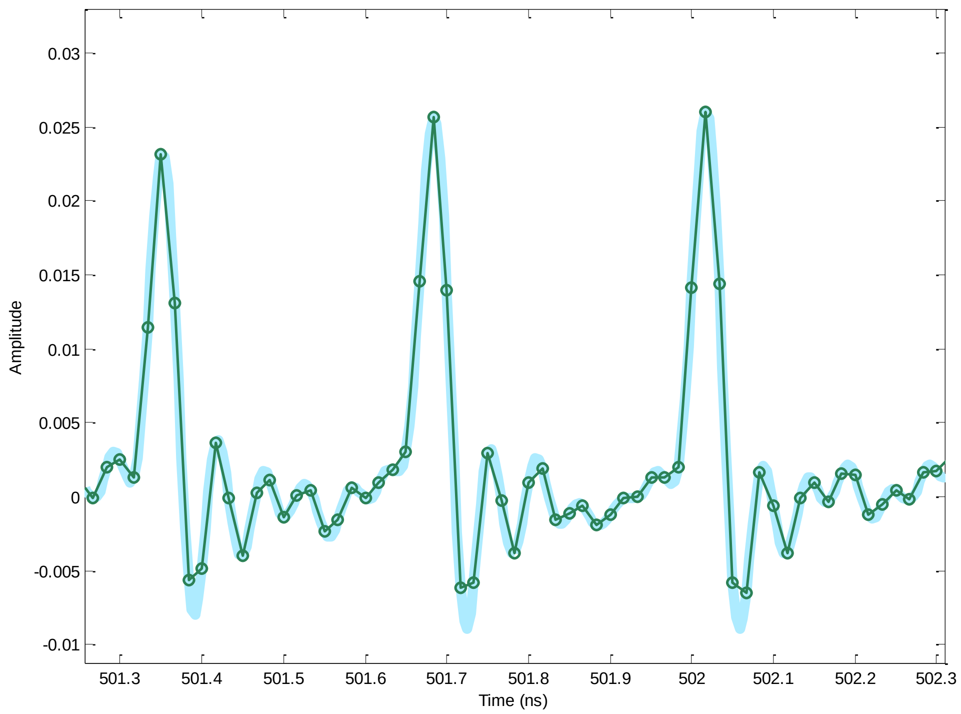

Figure 4.4.1.: An oscilloscope trace and four times sin(x)/x interpolation

This results in our 5.5 ps pulse appearing as a roughly 35 ps wide pulse (FWHM), with some oscillations after it. Also the sample rate is 60 GSamples/s, so it samples around every 16.7 ps this means that 4-5 points are recorded during a whole pulse. The interval accuracy is 1 ps (for a short duration such as 666 ps). (The trigger jitter is specified to be 2.5 ps RMS.) As mentioned earlier the jitter of the laser is about 0.5 ps RMS.

All this effectively results in the fact that the delay cannot be directly measured accurately. This can be solved by saving a trace and post processing using the following algorithm. The time of each pulse is recorded; a phase for each pulse is calculated using the oscilloscopes internal clock as reference. The average phase of the pulses from the attenuator arm is then subtracted from the average phase of the pulses from the delay arm.

This is a good method because with a large number of pulses the phase jitter of the laser pulses and the phase jitter of the sampling average out. Also the inaccuracy of the time base of the oscilloscope can be compensated for. This method works well both with the modulation on and the modulation off, the following description refers to the implementation of the latter, but the method can be easily applied to the former.

4.4.1 The algorithm in detail

A four times sin(x)/x interleaving is applied directly on the oscilloscope. The trace is saved and copied from the oscilloscope and processed on a PC with MATLAB. The trace is processed linearly. A trigger level is set. The first sample point above this level and the previous point are used, with a linear fit, to determine the time when the signal crosses the trigger level. From this time the pulses expected time, according to the oscilloscopes time base, is subtracted. The expected time of a pulse in this sense is the number of pulses so far times the nominal time between two pulses. The result of the subtraction is phase of the pulse. It is important to note that this is implemented in a way to avoid underflow even with a large number of pulses.

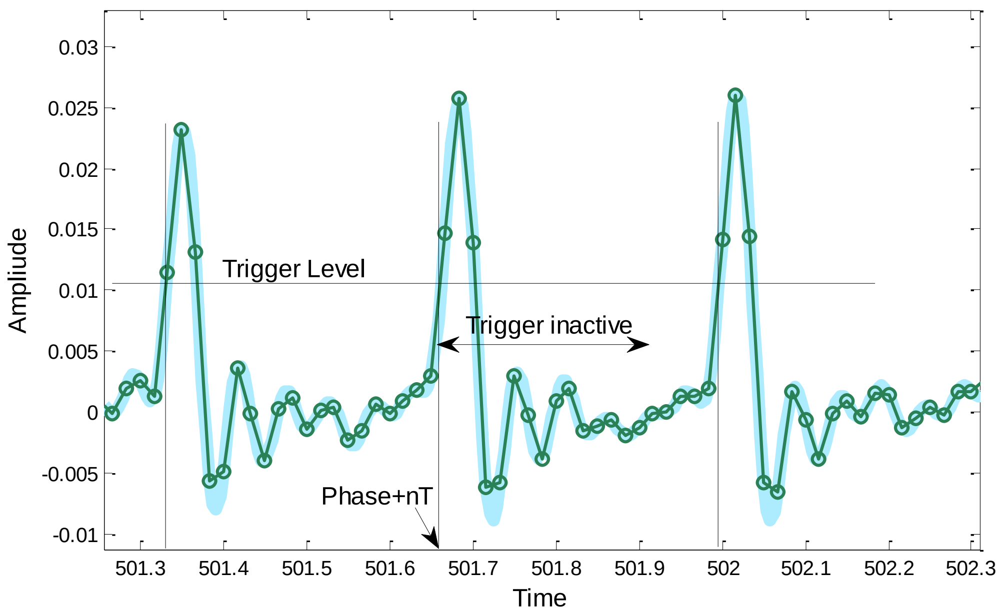

Figure 4.4.2.: A trigger event

Because the pulse repetition rate is not exactly 1.5 GHz and because the oscilloscope time base is not perfect the measured phase is constantly drifting in one direction. This can be corrected by applying a linear fit to the phase and then subtracting values of the fitted curve. The resulting corrected phases for the pulses from the delay arm and the pulses from the attenuator arm both follow more or less Gaussian distributions. The difference between the mean of these phases gives us the delay.

The difference in amplitude can also be measured by integrating the pulses from each arm separately, however this in more accurately done on phase coded signal.

The method described above can also be used with the modulation on; in this case it is important to use an equal and integer number of odd and even sub trains, as input.

5. Measurements

5.1 Phase-coding in operation, the signal along the path

The input signal is a 1.5 GHz repetition rate pulsed laser signal with 5.5 ps FWHM pulses. As previously mentioned the pulses seen on the oscilloscope through the photodiode appear much longer due to limited bandwidth. This and the relatively high amplitude noise can be observed in figure 4.4.1. Oscillations after the initial pulse can also be observed.

For the phase-coding to operate the modulators in the two arms need to be set to their operation point, and the delay between the timing signals needs to be set up. An excellent extinction ratio of around 40 dB can be achieved. This is shown on figure Figure 5.1.1. with the signal from the photodiode without signal shown in red.

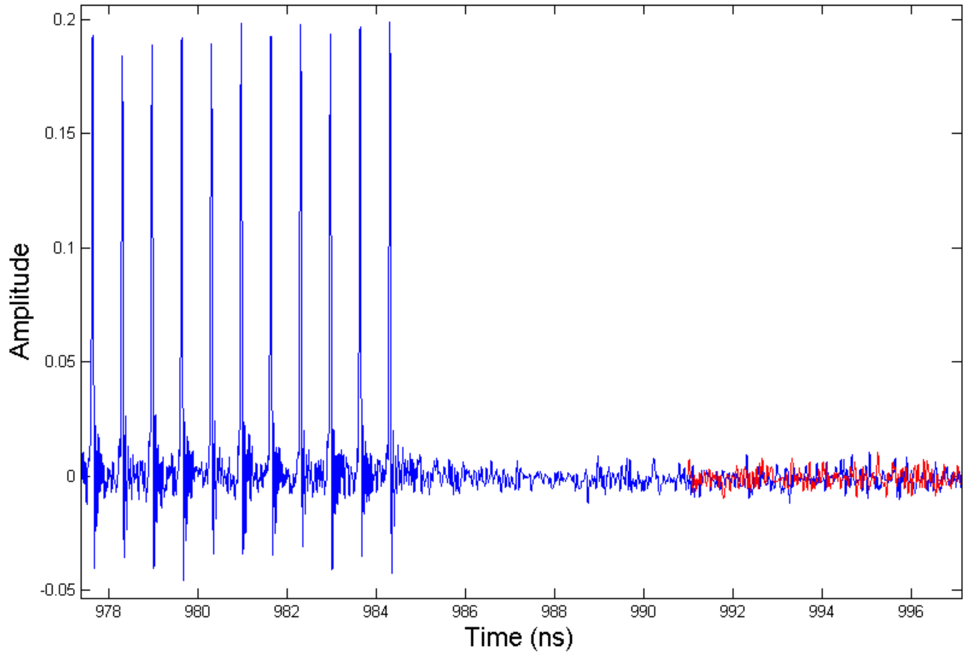

Figure 5.1.1.: The modulated signal from a single arm, and photodiode noise floor in red

Adding the two modulated signals together the in the combiner results in the phase-coded signal (figure 5.1.2.).

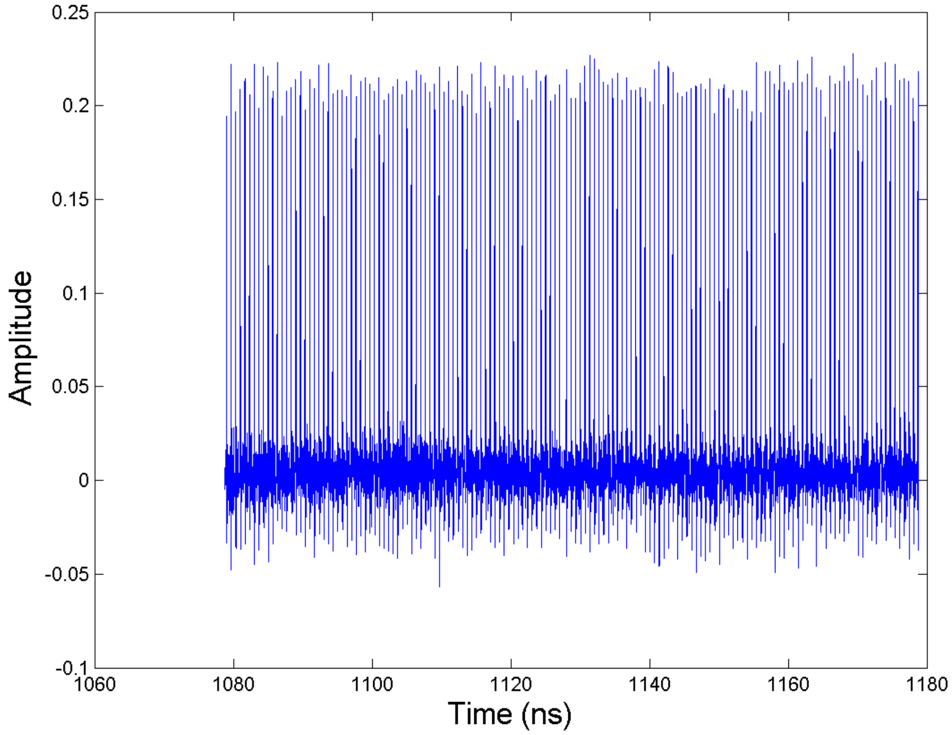

Figure 5.1.2.: The phase coded signal

To visualize the result the amplitude balance of the arm can be skewed, as seen on figure 5.1.3.

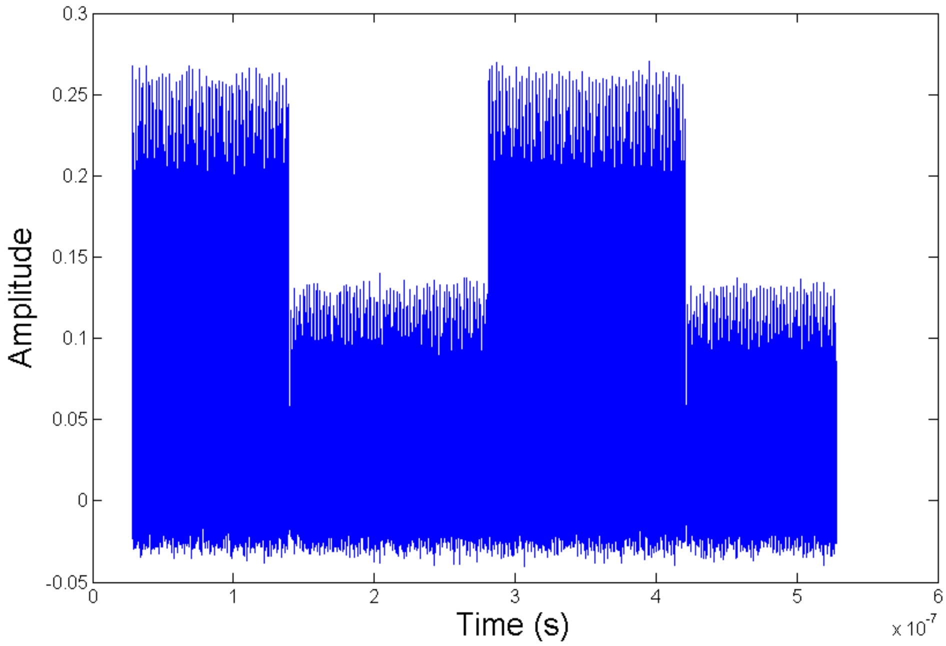

Figure 5.1.3.: The phase coded signal arms with the arms unbalanced

In the phase coded signal there are 333 ps and 1000 ps gap can be observed periodically, see figure Figure 5.1.4 and figure Figure 5.1.5.

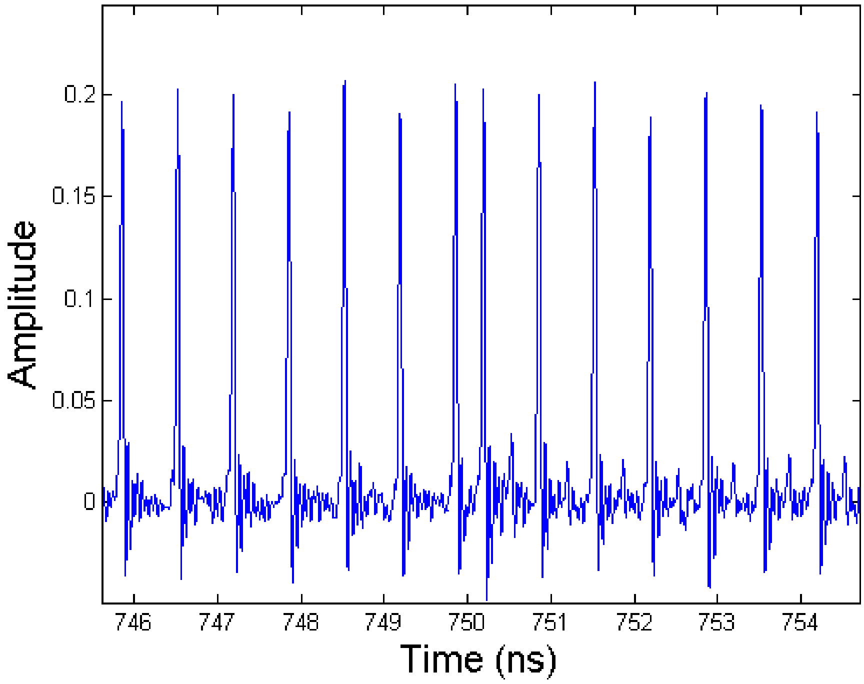

Figure 5.1.4.: The phase coded signal with a 333 ps gap

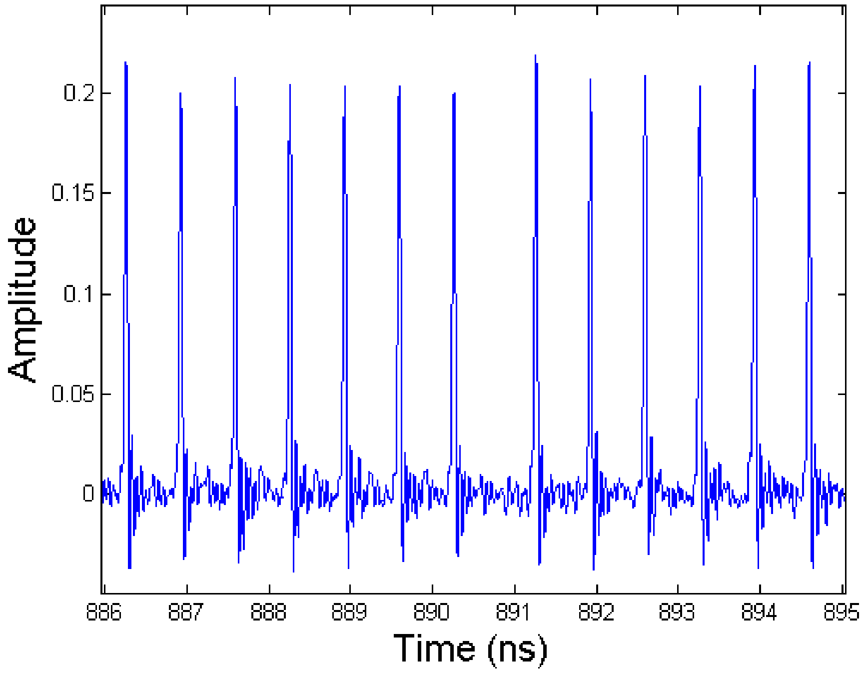

Figure 5.1.5.: The phase coded signal with a 1000 ps gap

As mentioned earlier the method using the spectrum analyzer is designed to be used with the modulators off and the time domain method is for both with or without modulation. The following measurements however where not carried out on coded signal, but with the modulators off in both cases. The resulting ~3 GHz repetition rate signal can be seen on figure Figure 5.1.6.

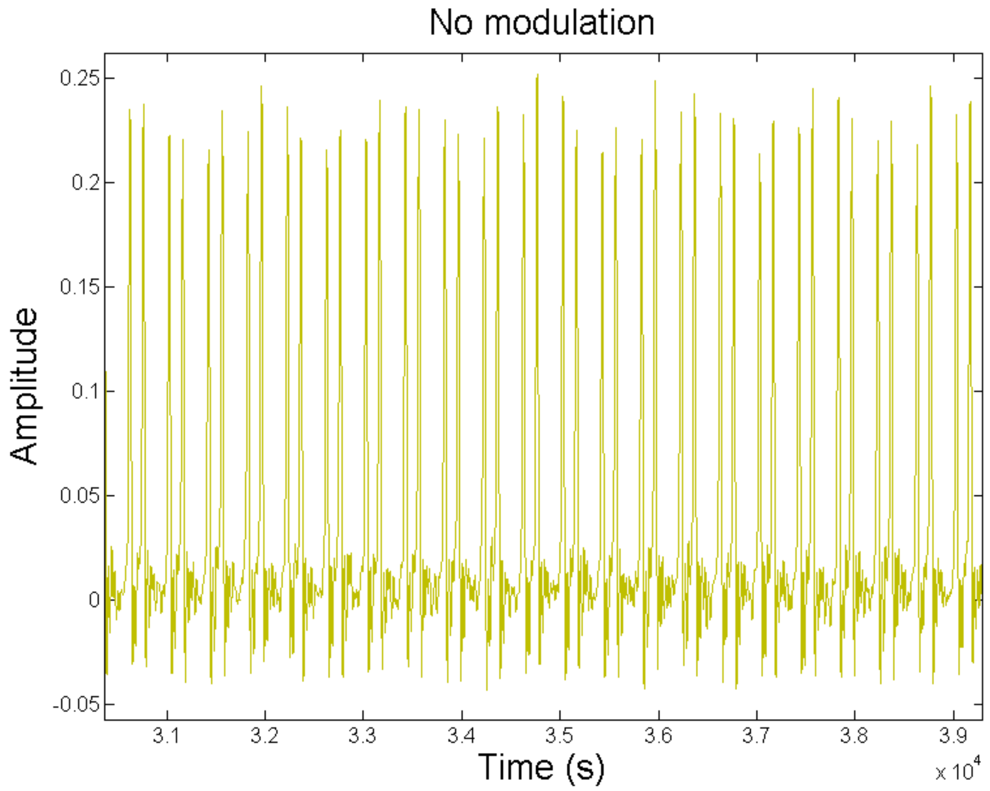

Figure 5.1.6.: An error in delay, causes a visible change in the pulse spacing

5.2 Measurements with spectrum analyzer

The first measurements where carried out with the frequency domain method, with the modulators not installed.

First let us consider a measurement from the 10th of October 2010. In this case the peak at 4.5 GHz was minimized by optimizing delay and amplitude balance. The 4.5 GHz peak was found to be a maximum of 38.7 dB under the 3 GHz peak.

Frequency	Signal (dBμV)
3 GHz	58
4.5 GHz	19.3
Noise floor	18

Table 5.2.1.

As first approximation; from equation (10) this ratio is equal to amplitude balance error if the delay error is zero. This results in at most a ~1.16% amplitude unbalance between the arms, if the delay error was zero. It is also possible to state that the timing delay error is at the most ~1.11 ps this being the case if the amplitude balance was perfect. This is a simple and quick way to estimate the difference from a single measurement point (plus reference).

Of course this can be done more exactly by varying the delay as seen on figure 5.2.1. The amplitude error in this measurement was constant, the attenuator was not adjusted, and the delay was changed by turning the delay screw.

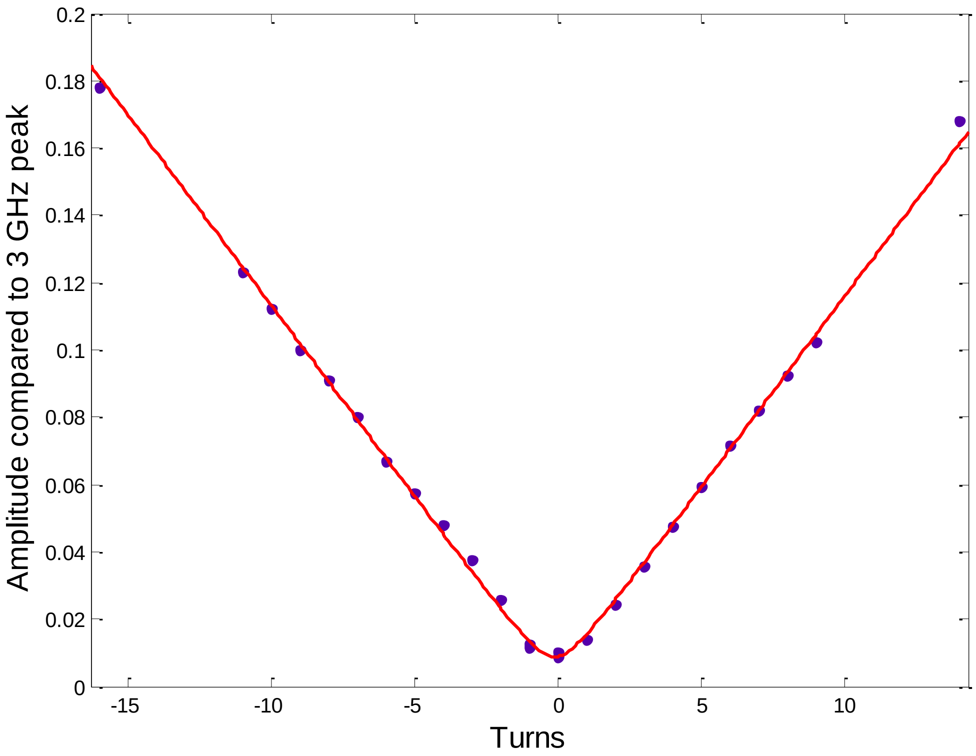

Figure 5.2.1.: Spectrum analyzer measurement and fitting

The fitting was done in MATLAB according to equation (9). The amplitude error was found to be 1.76% the delay error at the minimum was about 0.1 ps and the delay per turn of the delay micrometer 1.223 ps. This later value also verified with the oscilloscope and was found to be around 1.15 ps. The delay screw does not have a scale so the half turns are not exact.

The amplitude error measurement of 1% is rather high, this was due to the attenuator, its attenuation would drift with time. The relatively large drift meant that the attenuation would not stay exactly the same, at a higher error of 1% the drifts effect is less significant. Thus this larger amplitude error of less than 1% allows us to consider the attenuation roughly constant throughout the measurement. This drift also causes the amplitude of the 4.5 GHz peak to fluctuate slightly. In our experience the fluctuation increases as the peak decreases, this is at mostly due to the nonlinearity of the decibel scale, on the spectrum analyzer.

This first attenuator preformed badly and so was replaced by a new attenuator of the same model, and later using a variable neutral density attenuator wheel. Such an attenuator wheel is good for our application, because it is finely adjustable and provides a constant with the small beam size. (With a larger beam the attenuation would be different across the cross section of the laser beam.)

The attenuation can be set to higher accuracy for example on the 12th of October 2010, the 4.5 GHz peak was 67.15 dB below the 3 GHz reference. This corresponds to an amplitude error of 0.044% with no timing error or a timing error of 0.016 ps with no amplitude error. This was achieved with finer tuning of the attenuation and more light on the photodiode and different oscilloscope settings to decrease the noise floor.

Frequency	Signal (dBμV)
3 GHz	90.15
4.5 GHz	23
Noise floor	-3

Table 5.2.2.

In this case the achieved accuracy almost only limited by the accuracy of adjusting the attenuator and delay by hand. Of course this amplitude error may increases slightly if the attenuation drifts, but this suggests that phase-coding can be implemented to keep the amplitude error between pulses under 0.1%, as specified, if the input light has good stability. Unfortunately the addition of the modulators to the system greatly increases amplitude drift between the arms, if high temperature stability is not achieved.

5.3 Measurements with the oscilloscope

The used oscilloscope has a bandwidth of 18 GHz and a maximum sampling rate of 60 Gsamples/s as explained earlier this results in 4-5 samples per pulse. This is then interpolated with sin(x)/x interpolation to quadruple the number of samples. The measured signal is post processed and the delay time and amplitude unbalance is determined.

For a first example we will investigate the measurement of the 1st of December 2010. The delay line and amplitude balance was first set up with the spectrum analyzer and the oscilloscope was used to verify, the correctness of the setup. The delay was varied by half turns of the delay line screw. Then returning the screw to the initial delay position the setup was checked with the spectrum analyzer again.

After the initial setup the 4.5 GHz peak was found to be 49.6 dB under the 3 GHz reference, but at the end of the measurement it was only 26.6 dB under the reference due to amplitude drifts. From this we can conclude that the timing error is under 0.11 ps (from the initial value) and that the amplitude error is under 7.4% throughout the measurement. On figure 5.3.1. the measured delay can be seen as a function of the turns on the delay screw. Two methods are used for determining the delay: triggering on odd and even pulses on the same level and triggering on different levels for odd and even pulses. The use of two different trigger levels was required, because the amplitude error is so large in this case. The two methods are practically the same if the amplitude error is small as can be seen later.

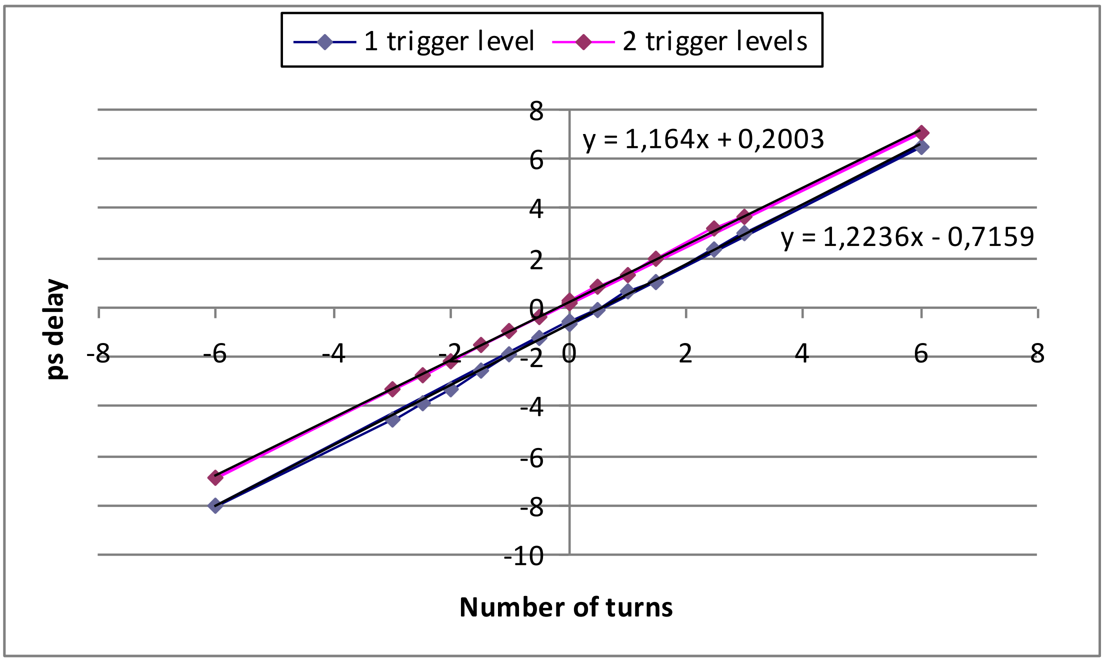

Figure 5.3.1.: Time domain measurement

The two methods give us the following parameters at the initial delay (train A and B mark the odd and even pulses grouped separately):

	Delay error	Phase jitter train A/B	Amplitude error	Amplitude noise train A/B
1 trigger level	0.551 ps	1.66 ps 1.55 ps	6.69%	5.08% 5.21%
2 trigger levels	-0.274 ps	1,66 ps 1,54 ps	6.81%	5.08% 5.21%

Table 5.3.1.

The delay error can be measured accurately despite the phase jitter due to the large number of pulses processed, almost 300,000. (This results in input file sizes of almost 360 MB, the size of the samples are limited by the memory of the machine and the size of arrays MATLAB can process.) The amplitude error is measured by integrating over a period around each trigger to sum the contribution of every pulse. This could be measured more accurately on the modulated train.

Since the signal is measured without modulation, the sign of the delay error cannot be determined, it is adjusted to fit the expected linear relationship between the number of turn and the delay error.

The measured delay error is slightly larger (-0.2 ps) than our expectation from the spectrum analyzer measurement, and the amplitude error is as expected (6.8%).

5.4 Measurements both in time and frequency domain

The first measurement of the 5th of April 2011 was done by setting up the delay with the spectrum analyzer and then varying the delay. After each turn on the delay line screw the amplitude balance was optimized with the spectrum analyzer, and the signal was measured both in the frequency and time domain.

This is advantageous because it is possible to keep the amplitude error low, and compensate for any drift that may occur. The attenuator wheel was used for this measurement, with the modulators in the system, but set to 100% transmission.

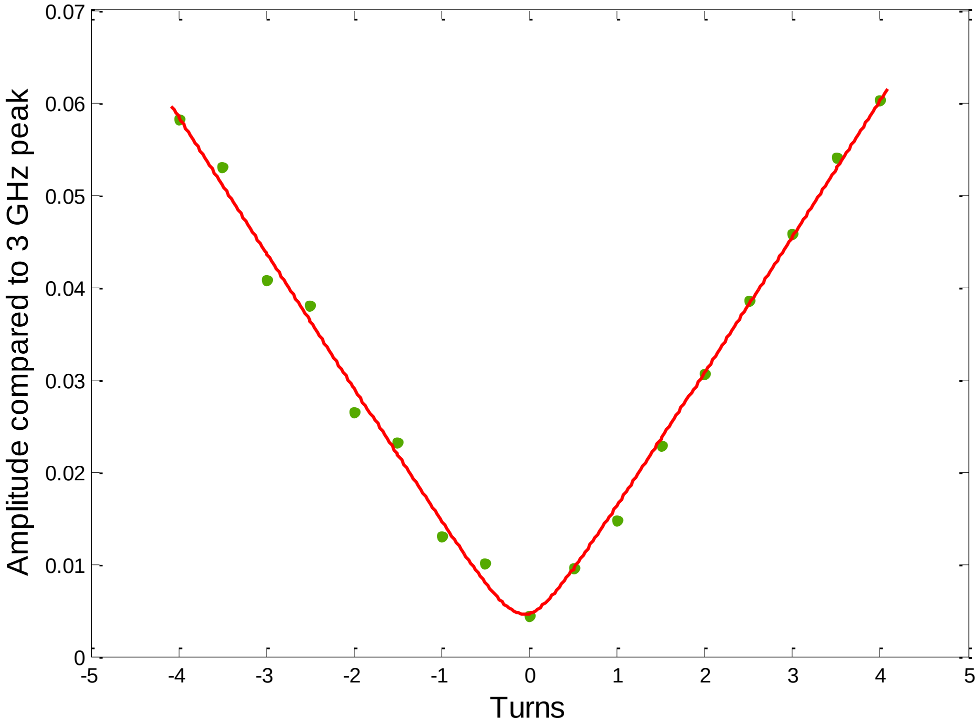

Figure 5.4.1.: Spectrum analyzer measurement and fittiong

The amplitude error was considered constant to be able to obtain a fit in MATLAB, this is not necessarily true, and so the quality of this fit is worse than in the previous example. The parameters of the fit are 0.9% amplitude error ~0.1 ps delay error at the minimum and 0.96 ps per turn of the delay line.

The signal level was 48 dB under the 3 GHz reference this corresponds to an amplitude error of 0.4% with no delay error or a 0.14 ps delay error with no amplitude error.

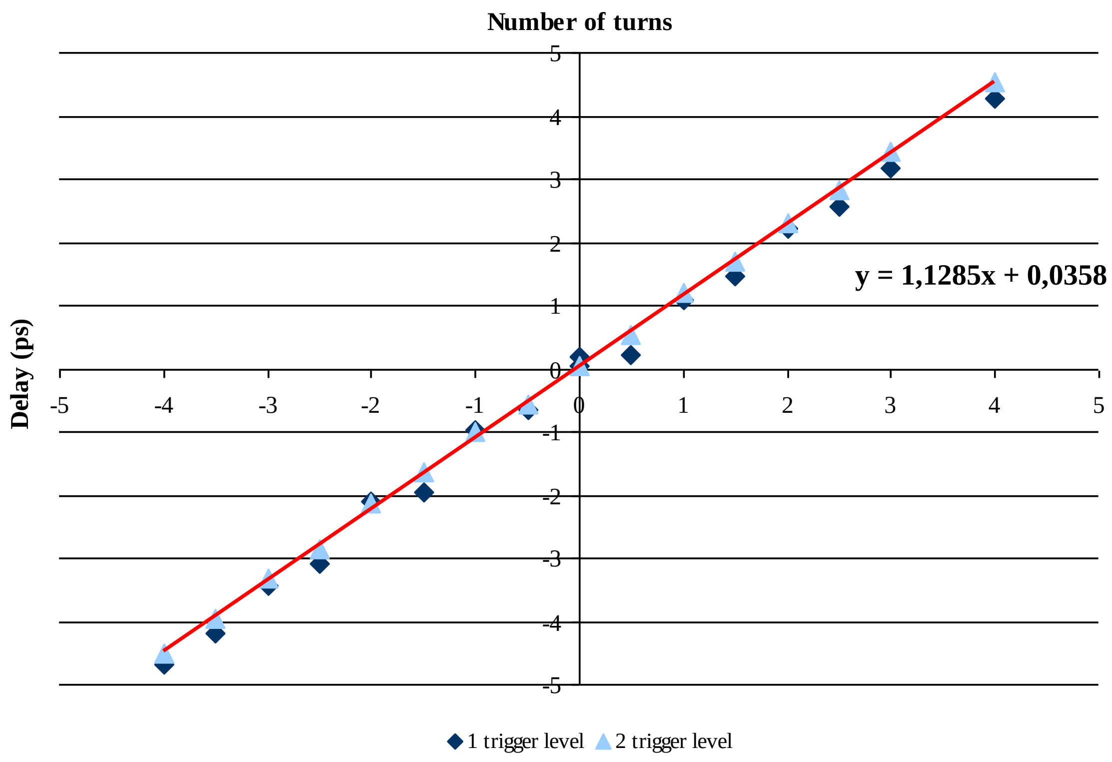

Figure 5.4.2.: First time domain measurement of the 5th of April 2011

Almost 80,000 pulses per point were processed in this measurement, but without interpolation.

	Delay error	Phase jitter train A/B	Amplitude error	Amplitude noise train A/B
1 trigger level	0.041 ps	0.86 ps 0.84 ps	0.65%	0.45% 0.45%
2 trigger levels	0.056 ps	1.66 ps 1.54 ps	0.53%	0.45% 0.45%

Table 5.4.1.

Both the delay and amplitude error are around our expectations from the spectrum analyzer measurement. The amplitude error is slightly higher then calculated but within expected accuracy, the accuracy of the amplitude measurement can be greatly improved by applying the same method to the phase-coded train.

The second experiment from the 5th of April 2011 was done slightly differently, after the initial setup the delay was varied, and after each change of the delay the signal was measured both on the oscilloscope and the spectrum analyzer, with the exception that the spectrum analyzer measurement was done on a wider range. Unlike in the previous experiment the amplitude balance was not changed throughout the experiment.

The 10.5 GHz peak was used for the spectrum analyzer measurements to demonstrate the increased delay sensitivity. At the initial setup the 10.5 GHz peak was 44.1 dB below the 9 GHz reference. This corresponds to a maximum of 0.6% amplitude error or a maximum delay error of about 0.19 ps.

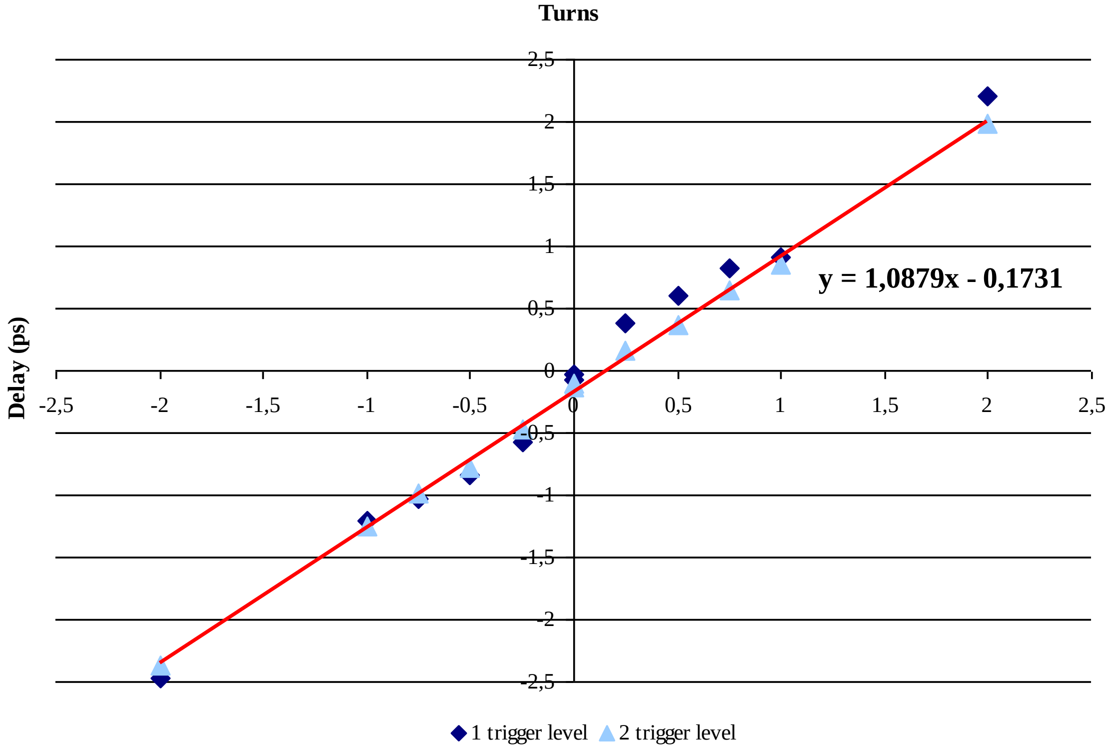

Figure 5.4.3.: Second time domain measurement of the 5th of April 2011

These measurements (seen on figure 5.4.3.) where done with 4 times interpolation and calculated from almost 300,000 pulses for each point.

	Delay error	Phase jitter train A/B	Amplitude error	Amplitude noise train A/B
1 trigger level	-0.027 ps	0.943 ps 0.925 ps	1.31%	1.32% 1.33%
2 trigger levels	-0.136 ps	0.924 ps 0.936 ps	1.31%	1.32% 1.33%

Table 5.4.2.

From the delay error and the amplitude error determined in the time domain the expected magnitude of the 10.5 GHz peak can be calculated, using equation (8).

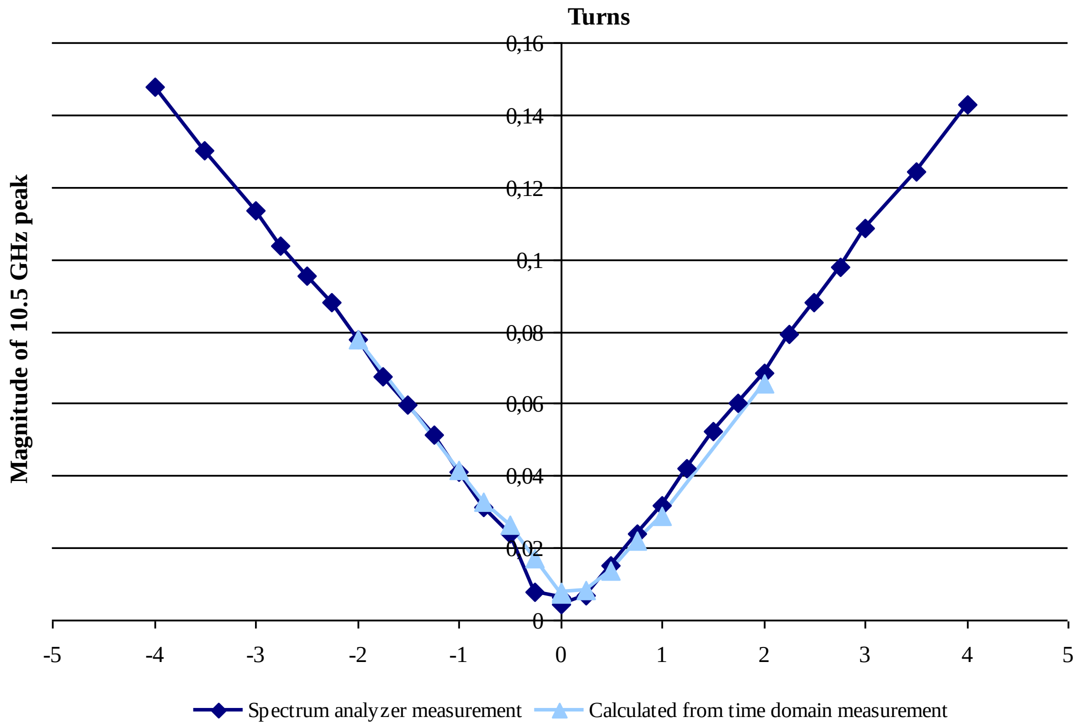

Figure 5.4.4.: Measured and calculated magnitude of the 10.5 GHz peak

As seen on figure 5.4.4. the calculated and measured values fit each other very well, except at -0.25 turns. The only other discrepancy between the two is at zero and plus a quarter turns. From this we can conclude that amplitude error measured in the time domain is larger than in reality. As mentioned before the accuracy of the amplitude error measurement can be greatly improved by applying this method to the phase-coded train.

5.5 Accuracy and other considerations

5.5.1 The frequency domain method

The frequency domain method is capable of setting the delay and amplitude balance to an accuracy significantly better than 0.1 ps and 0.1% as seen in the measurement of the10th of October 2010. The great accuracy can be achieved due to the high dynamic range of the spectrum analyzer. A great advantage of this measurement method is that noise such as detector noise generally increases the measured peak and thus makes our calculations of maximum amplitude balance and delay error conservative. The limiting factors are the increasing fluctuation of the measured peak with its intensity decreasing, the accuracy to which the delay and attenuator can be set. And most importantly the drift of the amplitude balance due to the attenuator and modulators.

The fluctuation of the peak is due to the amplitude and phase noise of the laser signal and the measurement error of the photodiode. The photodiode preformed surprisingly well, allowing us to decrease the 4.5 GHz peak more than 60 dB under the reference 3 GHz peak. But perhaps the most important cause of the fluctuation is the drift of the amplitude balance. The fluctuation is greater when the amplitude of the peak is smaller, this partly due to the nonlinearity of the decibel scale, and partly due to the fact that the fluctuation in an arm becomes more significant compared to the peaks average value as the peak gets smaller (the peak linearly increases with amplitude balance error if the timing error is small).

It is a very good sign that when adjusting the delay or amplitude the measured value changes very sensitively, this is further confirmation that the method works as expected.

The drift of the attenuators was a major problem, but this was solved by changing to the variable neutral density attenuator wheel. An other solution would have been to temperature stabilize the previous attenuator. However the drift of the modulators is more significant, these modulators where designed to keep there operating point stable with a feedback system, this system needs to be implemented for our application.

The calculation of maximum amplitude balance error with no timing error and maximum timing error with no amplitude balance error can be considered very good indicators of the accuracy of the setup. It can be safely assumed that the both errors are not significantly larger than these values. Varying the delay and measuring the 4.5 GHz peak results in a graph that fits well to our expectation as can be seen in the measurement of the 10th of October 2010. This provides a confirmation of our theoretical model. Unfortunately the fit does not provide much more information than the calculation of expected time and amplitude error from a single point.

5.5.2 The time domain method

In the time domain method a phase is determined for each pulse, a single such phase for each pulse train does not provide much information regarding the delay between the two pulse trains due to phase jitter and measurement error. The principle of the measurement is that with a very large number of pulses the measurement error decreases and the effect of phase jitter decreases.

The resulting delay error is actually calculated in phase with the pulse trains determining the frequency; and then is converted to picoseconds for convenience, from the pulse repetition frequency (1.5 GHz). This means that the result is independent of the oscilloscope time base.

The time domain measurement algorithm assumes a long sample with a large number of pulses. Each pulses phase is measured with a significant error, the RMS of the phase values in a single train is about is about 1-2 ps and the required accuracy is about 0.1 ps. So the goal is not to have any systematic error, and use a large number of pulses. This phase jitter comes from two sources the phase jitter of the laser pulses and the error of the measurement. The phase jitter of the laser pulses is specified to be under 0.5 ps, according to these measurements this could be more in reality. But the main source of the phase error is the phase error of the measurement, the phase error of the measurement is mostly caused by the amplitude noise and amplitude balance error.

To confirm that we have enough samples and our phase measurement is working properly, it is worth studying the histogram of the measured phases. We can expect a roughly Gaussian distribution. Even if the distribution is not Gaussian we would expect the distribution for the two trains from a single measurement to have the same distribution. The histogram of the phases of the trains from measurement of the 1st of December 2010 can be seen on figure 5.5.1. The measured delay error is 0.27 ps.

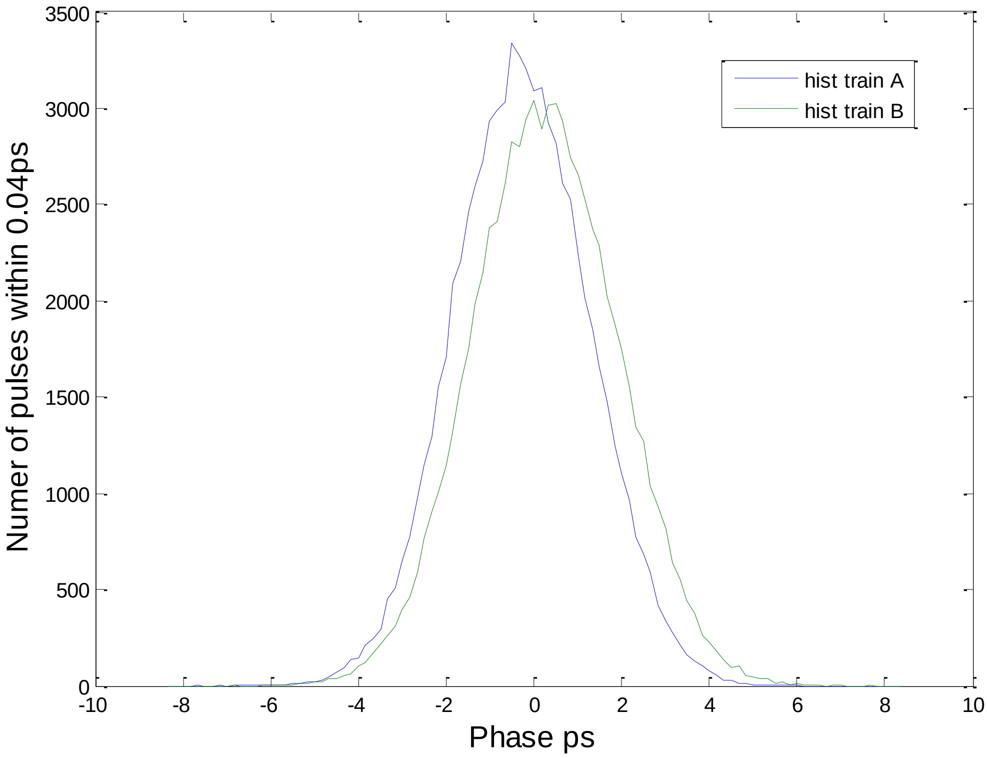

Figure 5.5.1.: Phase histograms at the initial delay setting the measurement of the 1st of December 2010

As we can see both distributions are roughly Gaussian as expected. If there would have been a pulse that would have been too small to trigger on or some other anomaly, we could observe some large phase error measurements in the bins on the edges of the histogram.

The algorithm also assumes that the pulses are identical in amplitude and shape. This causes substantial amplitude error, because smaller pulses appear delayed and larger pulses appear early. To further understand the measurement it is important to that essentially what we see on the oscilloscope output is the impulse response of the photodiode, bandwidth limited by the oscilloscope input filter which has a bandwidth of 18 GHz.

The measured amplitude of a pulse needs a dT time to rise before it triggers. As a first approximation we can model our pulse as having a straight rising edge as seen on figure 5.5.2. This means that the time of:

$$dT = \frac{\text{trigger level}}{\text{peak}} \cdot T_{rise} \qquad \textbf{(11)}$$

Passes before each trigger event this is however dependent on amplitude errors of the pulses. A typical dT would be about 10 ps with a trigger at 40% of the peak and a rise time of 25 ps. This is a very rough estimate but it gives us an idea of how much the amplitude variation effect the measured phase. For instance an amplitude error of 1% would cause a delay change of the magnitude of 0.1 ps.

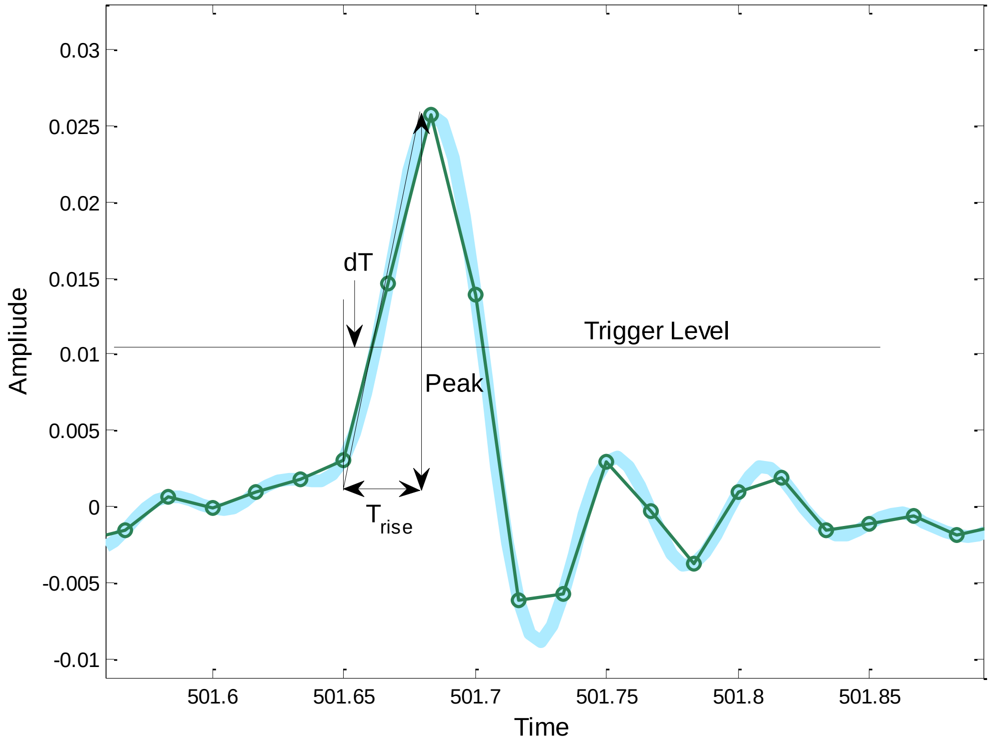

Figure 5.5.2.

This is the reason a different trigger level needs to be set for the two pulse trains. For instance in the second measurement of 5th of April 2011 the initial delay was -0.027 ps, taking into account the amplitude balance error of 1.31% and using two triggers the measured delay error changes to -0.136 ps this corresponds well with our estimated effect of amplitude difference which would be a change of 1.3 ps.

An other assumption made is that the oscillations after the pulses die away by the time the next pulse arrives, otherwise there can be coupling between the odd and even pulse trains. As seen on figure 4.4.1. the oscillations die almost completely by the next pulse. Such coupling could increase error, though with 0 ps delay error and 0% amplitude balance error the two trains disturb each other symmetrically. To avoid this problem only a part of the signal around the trigger is used tom determine the amplitude. This problem would be solved by applying the time domain method to the phase coded train, and the amplitude error would also be measured more accurately, using the effective values of whole sub trains to determine the amplitude balance.

The time domain method was not applied to the phase coded pulse train, because the phase-coding was only fully operational during and before an experiment known as the PHIN run. The PHIN experiment only runs for a few weeks a few times a year as the laser cannot be used to produce the main beam in CALIFES, at the same time. During the PHIN run laser time was crucial, and perfect setup was not yet important for the measurements in question. After the PHIN run the laser system was used in a different manner with booster amplifier – which is a fiber optic amplifier at the phase-coding output – incorporated into the system. So the phase-coding was not fully setup again, because of the time required.

6. Conclusions

The goal of this thesis was to develop a method to accurately set up the delay in the delay arm of the phase coding and the amplitude balance between the two arms of the phase-coding. The ultimate requirement for the phase coded laser beam is phase jitter of 0.1 ps and an amplitude stability of 0.1%.

A frequency domain method was developed, theoretically explained and experimentally investigated. Our experience shows that without the modulators and with a good attenuator a delay error and amplitude balance significantly better than the above parameters can be achieved (see: measurement of the 12^{th} of October 2010). Thus the developed method ensures that the measurement of the delay and amplitude balance is not a limiting factor for the phase-coding signal quality.

The requirements for an optimal stability and amplitude balance were also determined: the attenuator has to be very stable, and the modulators have to be improved by temperature and possibly implementation of feedback.

The advantage of this method is a real time visual feedback from the spectrum analyzer while manually adjusting the delay line and attenuator. This kind of optimization is a routine task in laser rooms.

A time domain method was also developed to verify the functionality and accuracy of the frequency domain method. This method does not provide a real time feedback. The algorithm could be ported to the oscilloscope, though processing a sample of 300,000 points can take several minutes with the current algorithm. This procedure provides us with a separate value for the amplitude balance and the delay error, unlike the previous method. The delay value determined from the oscilloscope trace was found to be not quite as accurate as the previous method but still accurate to about 0.1 ps or less at its best.

Unfortunately determining the amplitude balance using this method is not especially accurate, though it works quite as well especially at larger differences. This is due only partly to the limited accuracy of the oscilloscope. The main limit of the accuracy is the way the amplitude is determined: a small part surrounding the trigger is used. The measurement could be far more trustworthy if the method where applied to the phase-coded pulse train. This is how the method should be applied in the future.

The two methods where compared directly in the second experiment from the 5th of April 2011. The good agreement between the two results further confirms that the two methods work as expected.

7. References

[1] J. Ellis; A 3 TeV e^+e^- linear collider based on CLIC technology: Physics goals of the next century at CERN, CERN-2000-008, (2000), p. 1

[2] G. Geschonke; Technical description of the accelerator components: Explanation of the CLIC two-beam acceleration, CLIC conceptual design report (dry run), (2011), p. 25

[3] Roger Ruber; RF Acceleration Structures, Accelerator Physics Course Uppsala University, (2008 Autumn), p. 26

[4] CLIC study home page: http://clic-study.org/accelerator/CLIC-inaNutshell.php, (May 2011)

[5] B. Goddard; Feasibility demonstration of the CLIC technologies: Beam Transfer, CLIC conceptual design report (dry run), (2011), page: 120

[6] CTF3 home page: http://ctf3.home.cern.ch/ctf3/New_description.htm (May 2011)

[7] R. Corsini; An introduction to CTF3, CTF3 Meeting, (11th of February 2000)

[8] Dennis T. Palmer; The Next Generation Photoinjector, Ph.D. Thesis, (June 1998), p. 62

[9] H.H. Braun, E. Chevallay, S. Hutchins, et al.; The Photo-Injector Option for CLIC: Past Experiments and Future Developments, Proceedings of the 2001 Particle Accelerator Conference, Chicago, p. 720

[10] S. Döbert; Integration of the Phin RF Gun into the CLIC Test Facility, CLIC-Note-689, (2006)

[11] M. Csatari; Laser for CTF3 and Outlook for CLIC, International Workshop on Linear Colliders, (2010)

[12] CLIC Study Team; Proposals for Future CLIC Studies and a New CLIC Test Facility (CTF3), CLIC-Note-402, (1999), page 7

[13] MBC-1000 / MBC-1001 instruction manual, Photline Technologies, (March 2006)

[14] Encyclopedia of Laser Physics and Technology: http://www.rp-photonics.com/q_switching_instabilities.html (May 2011)

8. Special thanks

I would like to express my gratitude to Márta Csatári, who introduced me to the world of lasers, and taught me so much. And also to express my thanks for all the help she gave me throughout the whole process of this thesis work.

I would like to thank Valentine Fedosseev who gave me the opportunity to work in his section, in an inspiring scientific environment.

I would also like to thank Csaba Simon for his patients and attention in regards to this special subject.

And lastly I would like to thank CERN as an organization, for giving me the opportunity to work as a technical student, allowing me to participate in of one of the worlds most renowned scientific communities, at such a young age.

9. Appendix

9.1 The MATLAB code used in the time domain method

A built in MATLAB gui (graphical user interface) is used to select files to be processed. The procedure consists of several separate sections each clearing the memory loading the necessary data saved by the previous section, an saves the data. This strange structure was chosen to clear the memory of the unnecessary data from the previous cycle, and for debugging purposes. By saving intermediate results as well if something needs to be changed the, whole thing does not need to be recalculated.

```
interpRatio=4;

[filename, pathname] = uigetfile('*.mat', 'Select a QE
data','MultiSelect','on');

if ~iscell(filename)
    filename={filename};
    s=1;
else
    s=size(filename);
    s=s(2);
end

xlswrite('results.xls',{'1trigger','Phase','Phase jitter
RMS','','','Ampl','deviation (RMS)','','','2trigger','Phase','Phase
jitter RMS','','','Ampl','deviation (RMS)','','','';'Delay','Diff','A
','B','Both','Diff','A','B','Both','','Diff','A
','B','Both','Diff','A','B','Both','invert';},'raw','A1');

for i=1:s
    file=strcat(pathname,filename{i});
    mkdir(filename{i}(1:end-4))
    cd(filename{i}(1:end-4))
%|
%|Convert
%\________
interp=load(file);
save interp

%|
%|Preprocess
%\___________
clear all
clc

load interp

%plot(interp,'DisplayName','interp','YDataSource','interp','Marker','.
','MarkerSize',5);figure(gcf)
```

```
data=interp(24:end,1);%2);

data=data(1:end-mod(length(data),20*2*interpRatio));
plot(data(1:1000));

%test=2*mod([1:length(data)],80)-mod([1:length(data)],160);
%test=test/800;

save data data interpRatio

%|
%|Phase calc 1 trigger
%\_____________________
clc
clear all

load data

phaseelements=length(data)/(20*interpRatio)-200;
phase=zeros(phaseelements,1);
ampl=zeros(phaseelements,1);

compA=0.02;
%load AmplitudeRatio
compB=compA*1;%AmplitudeRatio;

i=20*interpRatio;
n=1;
while n<=phaseelements
    if (mod(n,2))
        comp=compA;
    else
        comp=compB;
    end
/-`1`18i9o    if (data(i)>comp)
        microphase=(comp-data(i-1))/(data(i)-data(i-1));
        macrophase=i-(n-1)*20*interpRatio;
        phase(n)=macrophase+microphase;

        ampl(n)=sum(data(i-4:i+10));

        n=n+1;
        i=i+15*interpRatio;
    else
        i=i+1;
    end
end

save longphaseamp1trigger phase ampl interpRatio

%|
%|Postproces 1 trigger
%\_____________________
clear all
%clc

load longphaseamp1trigger
```

```
phaseorig=phase;

Xphase=1:length(phase);
correction=polyfit(Xphase,phase',1);

phase=(phase-correction(2));

sub=Xphase*correction(1);
phase=phase-sub';

phaseA=phase(1:2:end);
phaseB=phase(2:2:end);

amplA=ampl(1:2:end);
amplB=ampl(2:2:end);

B=(mean(phaseA)-mean(phaseB))/(20*interpRatio)*(1/3*1000);

C=std(phaseA,1)/(20*interpRatio)*(1/3*1000);
D=std(phaseB,1)/(20*interpRatio)*(1/3*1000);
E=std(phase,1)/(20*interpRatio)*(1/3*1000);

F=(mean(amplA)-mean(amplB))/mean(ampl);

AmplitudeRatio=mean(amplB)/mean(amplA);
save AmplitudeRatio AmplitudeRatio interpRatio

G=std(amplA,1);
H=std(amplB,1);
I=std(ampl,1);

histA=hist(phaseA,-2:0.04:2);
histB=hist(phaseB,-2:0.04:2);
histX=(-2:0.04:2)/(20*interpRatio)*(1/3*1000);

save results1

%|
%|Phase calc 2 trigger
%\_____________________
%clc
clear all

load data

phaseelements=length(data)/(20*interpRatio)-200;
phase=zeros(phaseelements,1);
ampl=zeros(phaseelements,1);

compA=0.02;
load AmplitudeRatio
compB=compA*AmplitudeRatio;

i=20*interpRatio;
n=1;
while n<=phaseelements
    if (mod(n,2))
```

```
        comp=compA;
    else
        comp=compB;
    end
    if (data(i)>comp)
        microphase=(comp-data(i-1))/(data(i)-data(i-1));
        macrophase=i-(n-1)*20*interpRatio;
        phase(n)=macrophase+microphase;

        ampl(n)=sum(data(i-1*interpRatio:i+2.5*interpRatio));

        n=n+1;
        i=i+15*interpRatio;
    else
        i=i+1;
    end
end

save longphaseamp2trigger phase ampl interpRatio

%|
%|Postproces 2 trigger
%\_____________________
clear all
%clc

tic
load longphaseamp2trigger

phaseorig=phase;

Xphase=1:length(phase);
correction=polyfit(Xphase,phase',1);

phase=(phase-correction(2));

sub=Xphase*correction(1);
phase=phase-sub';

phaseA=phase(1:2:end);
phaseB=phase(2:2:end);

amplA=ampl(1:2:end);
amplB=ampl(2:2:end);


K=(mean(phaseA)-mean(phaseB))/(20*interpRatio)*(1/3*1000);

L=std(phaseA,1)/(20*interpRatio)*(1/3*1000);
M=std(phaseB,1)/(20*interpRatio)*(1/3*1000);
N=std(phase,1)/(20*interpRatio)*(1/3*1000);

O=(mean(amplA)-mean(amplB))/mean(ampl);

AmplitudeRatio=mean(amplB)/mean(amplA);
save AmplitudeRatio AmplitudeRatio interpRatio

P=std(amplA,1);
```

```
Q=std(amplB,1);
R=std(ampl,1);

histA=hist(phaseA,-2:0.04:2);
histB=hist(phaseB,-2:0.04:2);
histX=(-2:0.04:2)/(20*interpRatio)*(1/3*1000);

save results2

    load results1
    load interp;
    cd ..;
    A=filename{i};

xlswrite('results.xls',{A,B,C,D,E,F,G,H,I,'',K,L,M,N,O,P,Q,R},'raw',st
rcat('A',num2str(i+2)));
    cd(filename{i}(1:end-4))
    clear all
    load interp;
    cd ..

end
```